**US Army Corps
of Engineers**
Waterways Experiment
Station

Role of Expandable Clays
in the Environmental Fate
of Trinitrotoluene Contamination

by Steven L. Larson, Charles A. Weiss, Jr., M. Rochelle Martino, Jane W. Adams

DTIC QUALITY INSPECTED 1

19980909 036

Prepared for Headquarters, U.S. Army Corps of Engineers

The contents of this report are not to be used for advertising, publication, or promotional purposes. Citation of trade names does not constitute an official endorsement or approval of the use of such commercial products.

The findings of this report are not to be construed as an official Department of the Army position, unless so designated by other authorized documents.

REPRODUCTION QUALITY NOTICE

This document is the best quality available. The copy furnished to DTIC contained pages that may have the following quality problems:

- Pages smaller or larger than normal.

- Pages with background color or light colored printing.

- Pages with small type or poor printing; and or

- Pages with continuous tone material or color photographs.

Due to various output media available these conditions may or may not cause poor legibility in the microfiche or hardcopy output you receive.

☒ If this block is checked, the copy furnished to DTIC contained pages with color printing, that when reproduced in Black and White, may change detail of the original copy.

Role of Expandable Clays in the Environmental Fate of Trinitrotoluene Contamination

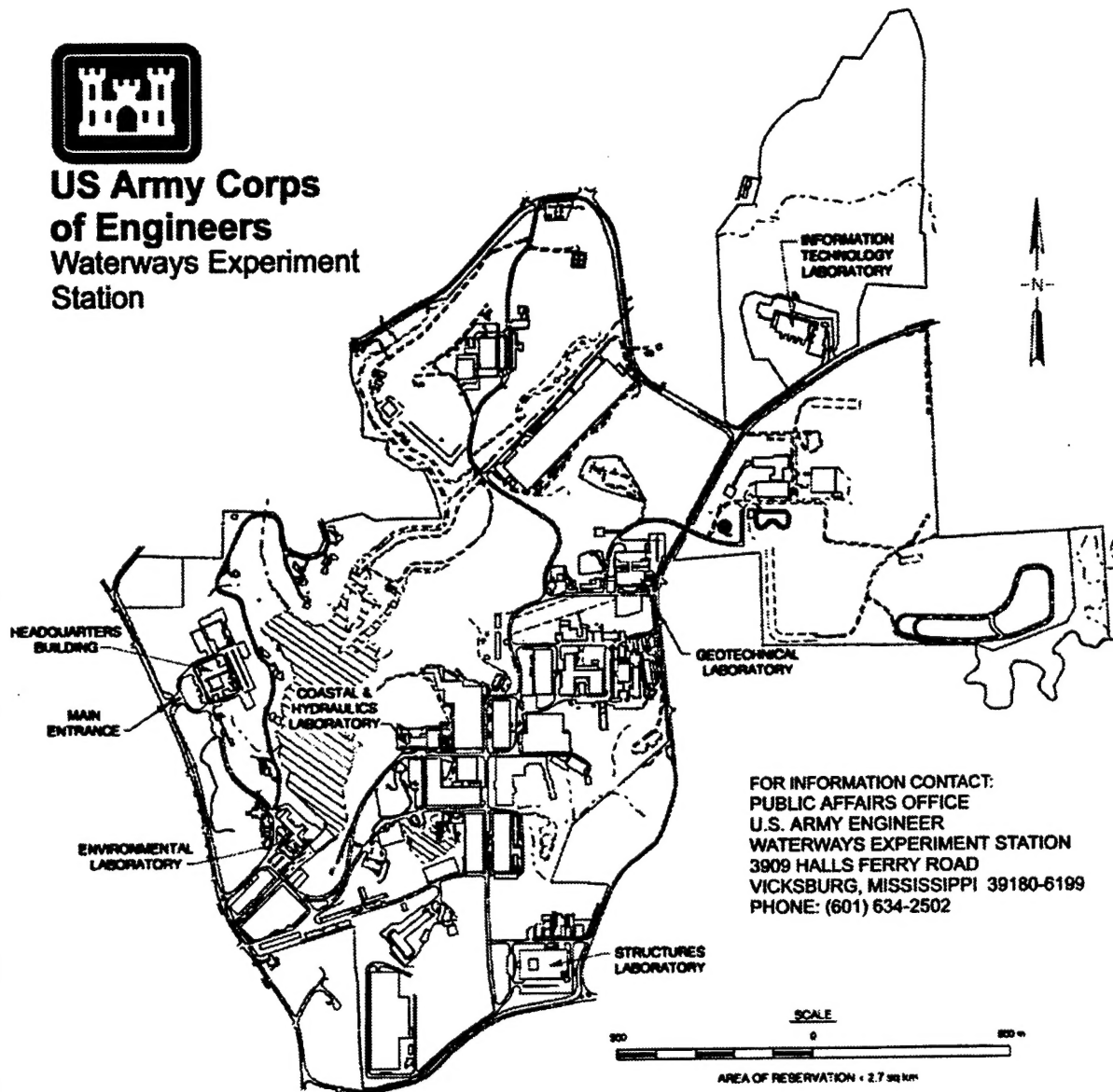by Steven L. Larson, Charles A. Weiss, Jr., M. Rochelle Martino, Jane W. Adams

U.S. Army Corps of Engineers
Waterways Experiment Station
3909 Halls Ferry Road
Vicksburg, MS 39180-6199

Final report

**US Army Corps
of Engineers**
Waterways Experiment
Station

FOR INFORMATION CONTACT:
PUBLIC AFFAIRS OFFICE
U.S. ARMY ENGINEER
WATERWAYS EXPERIMENT STATION
3909 HALLS FERRY ROAD
VICKSBURG, MISSISSIPPI 39180-6199
PHONE: (601) 634-2502

AREA OF RESERVATION < 2.7 sq km

Contents

List of Figures

List of Tables

Preface

The work reported herein was conducted by the Environmental Laboratory (EL) and the Structures Laboratory (SL), U.S. Army Engineer Waterways Experiment Station (WES), as part of the Installation Restoration Research Program (IRRP), the U.S. Army Environmental Quality Technology Program under Project BT-25 (Fundamental Effects of Soil Conditions on Spectral Signatures), and the Waterways Experiment Station Laboratory Director's Research Program (Chemical Models of Soil-Contaminant Interactions). Dr. Clem Meyer was the IRRP Coordinator at the Directorate of Research and Development, Headquarters, U.S. Army Corps of Engineers. Dr. M. John Cullinane, WES, was the IRRP Program Manager.

The study was conducted during FY96 and FY97 and the first quarter of FY98 under the general supervision of Dr. John Harrison, Director, EL; Mr. Norman Francingues, Chief, Environmental Engineering Division (EED), EL; Mr. Bryant Mather, Director, SL; and Dr. Paul Mlakar, Chief, Concrete and Materials Division (CMD), SL; and under the direct supervision of Dr. Ernesto Cespedes, Chief, Environmental Sensing Branch (ESB), EED, and Dr. W. Newell Brabston, Chief, Engineering Sciences Branch, CMD.

This report was prepared by Drs. Steven L. Larson, Environmental Chemistry Branch, EL, Charles A. Weiss, Jr., Engineering Sciences Branch, CMD, SL, and Jane W. Adams, ESB, EL. Technical assistance was provided by Mrs. M. Rochelle Martino, Engineering Sciences Branch, CMD. Technical reviews of this report were provided by Dr. John Curtis, ESB, and Mr. G. Sam Wong, Engineering Sciences Branch, CMD.

At the time of publication of this report, Director of WES was Dr. Robert W. Whalin. Commander was COL Robin R. Cababa, EN.

This report should be cited as follows:

Larson, S. L., Weiss, C. A., Jr., Martino, M. R., and Adams, J. W. (1998). "Role of expandable clays in the environmental fate of trinitrotoluene contamination," Technical Report IRRP-98-6, U.S. Army Engineer Waterways Experiment Station, Vicksburg, MS.

1 Introduction

Knowledge of the fate and mobility of explosives, by-products of explosives manufacture, and the degradation products of explosives in the environment is required to assess the risks associated with soil and water contamination by these compounds (Haderlein and Schwarzenbach 1993; Haderlein, Weissmahr, and Schwarzenbach 1996; Leggett 1985; Pennington 1990). The mobility of organic contaminants in groundwater is dependent on the properties of these contaminants and the media in which they are dispersed (Ukrainczyk and Rashid 1995; Pusino, Gelsomino, and Gessa 1995; Pusino, Petretto, and Gessa 1996; Karickhoff 1981; Bowman 1973; Bowman and Sans 1977). Sorption from an aqueous solution to solid surfaces is a key factor in predicting the behavior of hazardous compounds in the environment. In order to understand the interactions between explosive-based contaminants and clay soil components, a series of experiments were performed using smectitic clays and a 2,4,6-trinitrotoluene (TNT) degradation product, 2,4,6-triaminotoluene (TAT).

The adsorption and desorption of contaminants onto and from soil components is an area of concern for those interested in environmental risk assessment and remediation (Adams, Larson, and Weiss 1997). Understanding the interactions of contaminants with soil components is fundamental to the accurate prediction of in situ contaminant behavior. Modeling the movement of contaminants in groundwater usually assumes no soil/contaminant interactions. This assumption results in drastically overestimating the mobility of contaminants that interact with soil components (Karickhoff 1981; Pusino, Petretto, and Gessa 1996; Theng, Greenland, and Quirk 1967; Ukrainczyk and Rashid 1995). These interactions can affect not only the mobility of explosives, but also the bioavailability of contaminants to biosystems (including microbes, insects, plants, and animals). Contaminants that become strongly bound with soil components are less readily accessed by these systems. This has been observed in studies in which the extractability of contaminants from aged soils has been compared with freshly spiked soils (Pennington 1990; Jones 1996). The toxicity of the same concentration of a given contaminant appears to vary widely with the extent of soil/contaminant interaction (Alexander 1995).

The significance of soil contaminant interactions takes on more importance when the catalytic properties of mineral surfaces are taken into account. Purified mineral species are used extensively in pharmaceutical and industrial chemical

processes to facilitate molecular transformations (Pusino, Petretto, and Gessa 1996; Mercier and Detellier 1995; del Hoyo, Rives, and Vicente 1996). Naturally occurring mineral surfaces also act as templates on which molecular transformations can occur (Kunyima et al. 1990; Ernsten 1996; Klausen et al. 1995). This phenomenon has an impact on the risks associated with soil and sediment contamination, the natural attenuation of this contamination, and the treatability of contaminated soils and sediments.

Systems including both microbes and plants have been shown to degrade environmental contaminants with greatly reduced cost compared to traditional remediation techniques (Crocker, Guerin, and Boyd 1995; Carpenter et al. 1978; Hatzinger and Alexander 1995). One key to an effective bioremediation process is the mass transfer of contaminants to the microbial consortium for degradation, because often some fraction of the contaminant is rendered unavailable for biodegradation (Alexander 1995). Based on a fundamental understanding of the nature of site specific soil/contaminant interactions, estimations concerning the effectiveness of biotreatment can be made. Likewise, selection of the remediation technology with the greatest cost/benefit ratio can be made prior to implementation based on the nature of the contamination and the extent of contaminant sequestration by soil components.

The fact that extensive sorption of explosives residues to soil components occurs is well established. Studies have shown that nitroaromatic residues can be extremely resistant to removal from soils, with as much as 20 to 50 percent of radio-labeled explosives found to be associated with the soil compartment in controlled degradation studies with low mineralization to CO_2 or volatile organic compounds (Pennington 1990). This suggests that adsorption of explosives onto soil components renders them unavailable to conventional extraction methods. The nonpolar parent compound, trinitrotoluene, is not expected to adsorb to polar, clay-based soil components. It has been suggested that adsorption of TNT to soil components is a result of association of the contaminant with the naturally occurring organic components of the soil (Jenkins 1989). Figure 1 shows that the amination of successive nitro groups prior to ring cleavage in the reductive degradation of TNT results in formation of ionizable amino substituents. These aminated degradation products of trinitrotoluene have been detected in soil and water samples from contaminated areas (Jones 1996, Jenkins 1989, Leggett 1985).

The products of reductive degradation of trinitrotoluene, however, are ionizable. The organic cations on these molecules can possibly ion exchange with inorganic cations in clay-based soil components. The degradation product in which all three nitro groups have been reduced to amino groups is the most easily ionized to form a cationic compound. It is the interaction of this compound with expandable clays that is of interest, with respect to the fate of the "lost" material in radio-labeled studies.
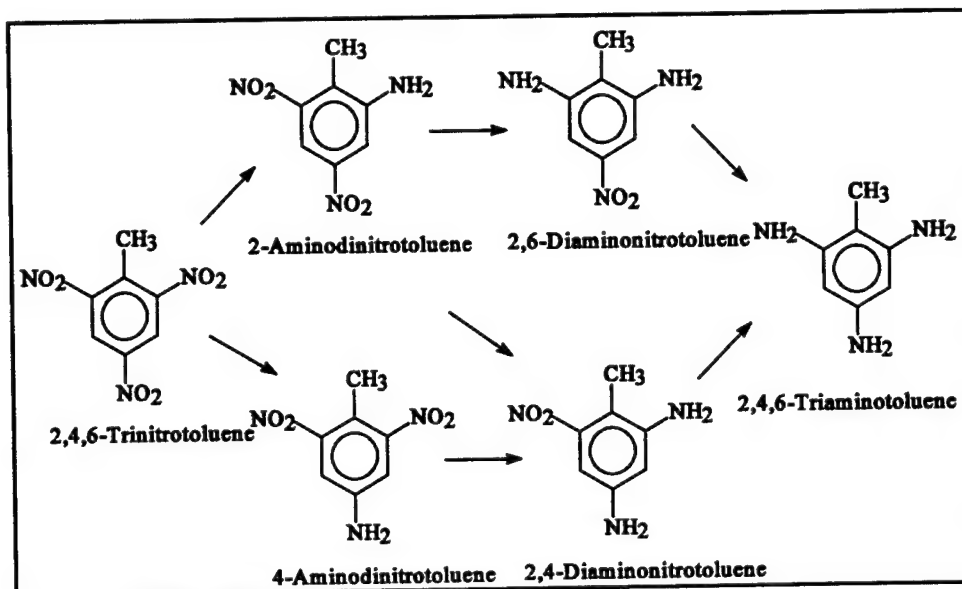
Figure 1. TNT reductive degradation pathway prior to ring cleavage

Sites for cation or species exchange on 2:1 clay minerals (e.g., illite, vermiculite, and smectites) include basal surface, edge-interlayer, and internal-interlayer sites. Cations or other charged species are adsorbed onto clays to balance negative charge on the phyllosilicate structure. This negative charge is caused by substitution of lower charged cations for those more highly charged in the tetrahedral or octahedral sheets. For hectorite and montmorillonite, charge is developed due to the cation substitutions (Li^+ for Mg^{2+} in hectorite and Mg^{2+} for Al^{3+} in montmorillonite) in the octahedral sheet. For saponite, charge development occurs due to Al^{3+} for Si^{4+} substitution in the tetrahedral sheet. Commonly, small cations (Na^+, K^+, Ca^{2+}, etc.) are adsorbed onto these clay minerals to passivate the negative charge on the structure. These cation exchange sites are illustrated in Figure 2 which shows the clay structure of expandable clays with layers made up of Si-based tetrahedral (T) and aluminum-based octahedral (O) sheets with interlayer cation exchange sites.

Broken bonds on the edges of crystallites may also cause development of a small charge. Because 2:1 expandable clays are an important and common component in natural soils that account for a majority of cation adsorption, adsorption of TAT is investigated for a series of pure homoionic smectitic clays (MacEwan and Wilson 1980).
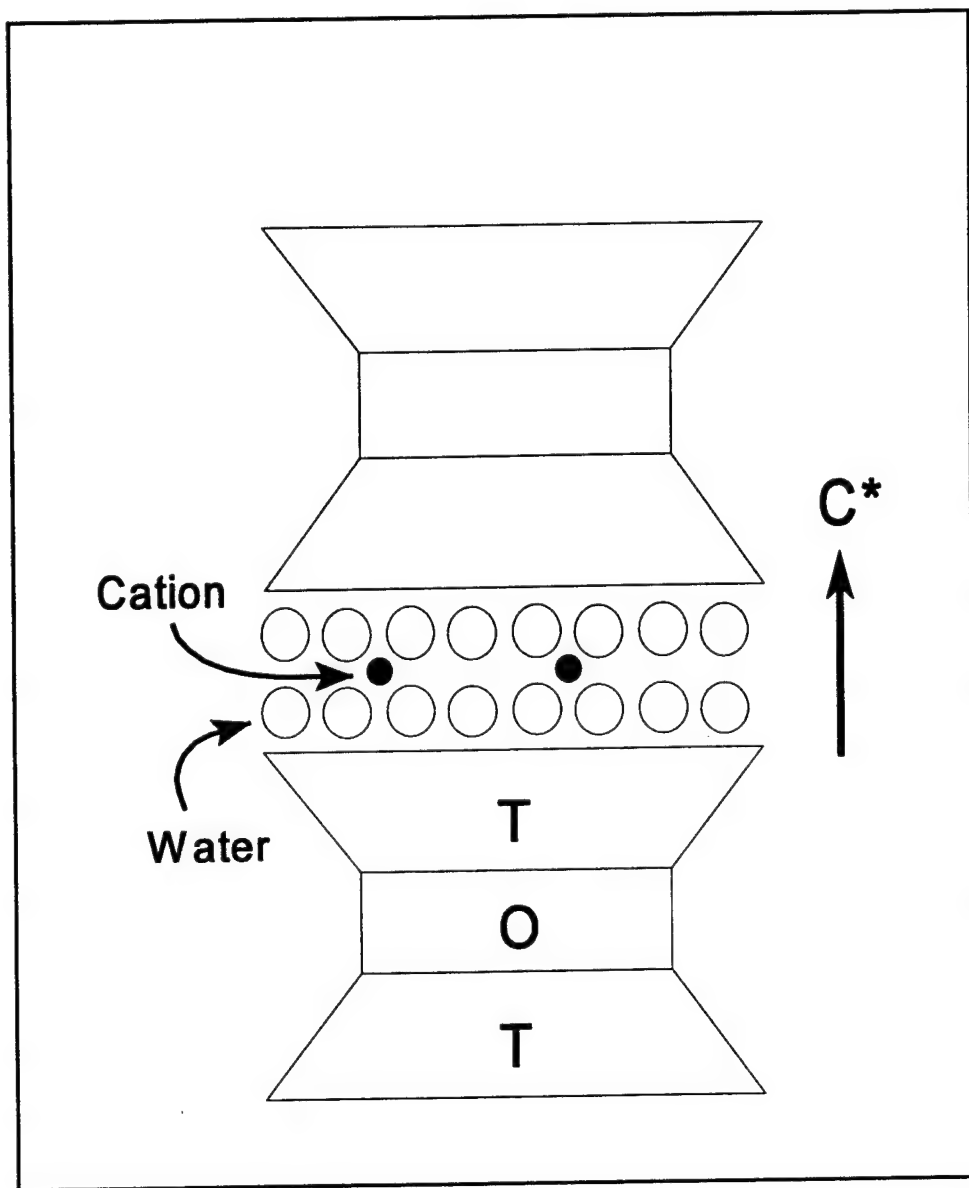
Figure 2.   Expandable and nonexpandable clays cation exchange sites

2   Experiment

Materials

Standard clay samples (smectites) obtained from the Clay Minerals Society Source Clay Repository, Columbia, MO, include STx-1, SAz-1, SHCa-1, SapCa-1, SWy-1, and SWa-1. An additional smectite (A.P.I. #27) from Belle Fourche, SD, was obtained from Ward's Natural Science Establishment, Rochester, NY, and assigned the sample name SBF-1. The smectitic clays used in this study are presented in Table 1.

Table 1 Mineral Type, Locality, and Sample Name for Smectites (<1µm size fraction)		
Mineral	**Locality**	**Sample**
Montmorillonite	Belle Fourche, SD	SBF-1
	Gonzales County, TX	STx-1
	Arizona	SAz-1
	Crook County, WY	SWy-1
Hectorite	Hector, CA	SHCa-1
Saponite	Ballarat, CA	SapCa-1
Nontronite	Grant County, WA	SWa-1

Preparation of <1 µm Clays

The seven clays listed in Table 1 were suspended in distilled water, placed in centrifuge tubes, and spun at 76 g's for 5 min. The <1 µm fraction was decanted and centrifuged at 76 g's for an additional 5 min. This process was repeated until there was no residue remaining in the centrifuge tubes. Following the initial sizing at 76 g's, the <1 µm fraction obtained was then spun at 7,606 g's for 1 hr, followed by collection and drying of the residue in a 50 °C oven overnight. The dried product was then milled to reduce the size.

Preparation of Sodium-Saturated Clays

A slurry of the <1 μm clay was suspended in 0.1 molar (M) sodium chloride in distilled water. The solution was placed in centrifuge tubes and spun at 7,606 g's for 1 hr. The supernatant was discarded and the residue resuspended in 0.1 M sodium chloride solution. This process was repeated four times. The sample was then washed by suspending the sample in deionized (DI) water and centrifuging at 7,606 g's for 1 hr. This washing process was repeated four times. Following the final wash, the sample was suspended in a minimum of DI water and dried in a 50 °C oven overnight. The dried product was then milled to reduce the size. In order to perform x-ray diffraction (XRD) analysis of the clay-size fraction (<1 μm), a slurry was suspended on a substrate of silicon and allowed to dry overnight at ambient room temperature. XRD analysis was used to verify the presence of Na^+ as the predominant cation present in the clay samples.

Preparation of TAT/Smectite Organo Clays

Organo clays were prepared by placing sodium-exchanged clays in contact with solutions containingTAT.[1] For the investigation of the TAT loading level on clay properties, clays were prepared by allowing a range of TAT to adsorb to a 40-mg sample of sodium-exchanged Texas montmorillonite (STx-1) and sodium-exchanged Wyoming montmorillonite (SWy-1). Two concentrations of TAT solution (20 and 300 ppm 2,4,6-triaminotoluene hydrocholride (TAT-$(HCl)_3$)) were prepared. These solutions were used to obtain organo clays at 14 TAT/clay ratios: 0.000, 0.002, 0.004, 0.006, 0.01, 0.023, 0.052, 0.100, 0.120, 0.200, 0.300, 0.600, 1.100 (SWy-1) and 1.500(STx-1) mg TAT/mg clay. Another set of organo clays was prepared by allowing TAT to be adsorbed onto the seven purified clays. Forty milligrams of sodium-exchanged clay was treated with a TAT solution cpontaining 300 ppm TAT-$(HCl)_3$. Two loading levels were prepared, one at 12 mass percent, 40 mg of sodium-exchanged clay with 16 ml of the 300 ppm TAT-$(HCl)_3$ solution. The other loading level representing TAT-saturated clays[2] was prepared by treating the 40-mg clay samples with aqueous TAT solution until TAT could no longer be adsorbed. The TAT solutions were adsorbed onto the clays by adding liquid to the clay sample, vortexing to achieve a clay suspension, and agitating for 18 hr to simulate a short-term exposure. The

---

[1] Because of the rapid rate of adsorption of TAT by smectites, complete adsorption is assumed at levels below saturation. This is confirmed by complete de-coloration of TAT solutions following centrifugation.

[2] In the loading experiments performed in this study, the contact time for TAT loading was fast (high aqueous concentration and short contact times) compared to loading as it occurs in the environment (low aqueous concentration and long contact times). For this reason what is termed "TAT-saturated clay" in this report refers to the degree of saturation produced by the experimental methods as described above. Utilizing another loading scheme may result in a significantly different maximum mg TAT/mg clay ratio.

samples were centrifuged for 10 min at 684 g's to separate the solid fraction[1] which was then analyzed by XRD.

XRD Analysis

XRD samples were prepared as follows: a slurry of the clay sample with water was mixed, suspended on a substrate, and dried overnight. A Philips PW1800 Automated Powder Diffractometer system was utilized to collect XRD patterns employing standard techniques for phase identification. The run conditions included Cu Kα radiation and scanning from 2 to 65° 2θ with collection of the diffraction patterns accomplished using personal computer-based Windows 95 versions of Datascan (Materials Data, Inc.) data acquisition software and Jade X-ray diffraction analysis software. Calculation of clay geometry (d-spacings) from the scan angle (2θ) is given by Bragg's Law (Moore and Reynolds 1989), $n\lambda = 2d\sin\theta$, where n is a positive integer, and λ is the wavelength of the excitation radiation (for Cu Kα = 1.54 Å = 0.154 nm).

Fourier Transform-Infrared Spectroscopy

Fourier Transform-Infrared (FTIR) spectroscopic measurements of the soils were obtained over the range from 4,000 cm^{-1} to 400 cm^{-1} (2.5 to 25 µm) at 4 cm^{-1} resolution using a Nicolet 740 FT- IR spectrometer. Samples were prepared by the potassium bromide (KBr) pellet method using an agate mortar and pestle and then cold pressing in a press to make a thin, transparent pellet. All measurements were made in N_2 at room temperature. Data collection proceeded 2 hr after placement in the spectrometer to allow flushing of atmospheric H_2O. Experiments were made using 32 scans at 4 cm^{-1} resolution after determining that higher resolution and increased scans did not significantly improve the signal-to-noise ratio. All data collected in this study were interpreted using Nicolet automatic spectrum-processing routines.

---

[1] The clays tend to flocculate after exposure to small quantities of TAT. The formation of this floc sllowed the use of a significantly lower centrifuge speed.

3 Results and Discussion

Changes in Interlayer Spacing
Under Varied TAT Loading

A series of organo-clays were prepared as previously described using Texas and Wyoming montmorillonite smectites (STx-1 and SWy-1) and a TAT solution. Increasingly greater amounts of TAT were allowed to exchange onto the initially sodium-saturated <1 μm sized clay. Tables 2 and 3 show the mean d(001) peak position[1] (the height of a single clay layer-interlayer-clay layer unit) and the interlayer expansion as a result of TAT loading onto the clay.

Table 2 Loading of TAT onto Sodium-Exchanged Texas Montmorillonite (STx-1)		
mg TAT/mg Na-STx-1	d(001) Peak Position, nm	Interlayer Expansion, nm
0.000	1.318	0.000
0.002	1.271	-0.047
0.023	1.289	-0.029
0.052	1.348	0.030
0.100	1.369	0.051
0.120	1.391	0.073
0.300	1.591	0.273
1.500	1.577	0.259

---

[1] The mean d(001) peak position is operationally defined as the point (angle) between 3.5 to 8.5 °2θ at which the peak area is bisected. That angle is then used to calculate the d(001) distance. This convention was adopted as a result of the increased peak asymmetry with increased TAT loading levels.

Table 3
Loading of TAT onto Sodium-Exchanged Wyoming
Montmorillonite (SWy-1)

mg TAT/mg Na-SWy-1	d(001) Peak Position, nm	Interlayer Expansion, nm
0.000	1.262	0.000
0.002	1.235	-0.027
0.023	1.262	0.000
0.052	1.265	0.003
0.100	1.299	0.037
0.120	1.308	0.046
0.300	1.424	0.162
1.100	1.413	0.151

Figures 3 and 4 show the superimposed diffraction patterns collected for the series of typical TAT-exchanged smectites. As can be seen, increased loading of the TAT onto the clay resulted in successive shifts of the d(001) peak position which correspond to expansion of the interlayer spacing. This change in clay geometry is due to replacement of the spherical sodium ions in the interlayer with the asymmetrical ions associated with the triaminotoluene.

A plot of the change in interlayer spacing (from the sodium-exchanged sample) in nanometers with respect to the ratio of the mass of TAT adsorbed in milligrams to the mass of clay present is presented in Figures 5 and 6. Three distinct behaviors were observed: (1) an initial decrease in d(001) spacing with the adsorption of small amounts of TAT (<0.2 percent by mass), (2) a roughly linear increase in d(001) spacing with respect to the amount of TAT adsorbed at higher concentrations (between 0.2 and approximately 25 percent), and (3) no variation in d(001) spacing at TAT loadings greater than 30 percent. A maximum d(001) spacing was achieved at between 1.4 and 2.0 nm, depending on the clay type.

Variation of TAT Adsorption
by a Series of Purified Clays

In order to better understand the process of TAT loading onto clay surfaces, TAT exchange experiments were performed on a number of purified, sized, and sodium-exchanged smectitic clays. Each clay type was analyzed using XRD on ordered samples with three cation loadings. Table 4 lists clay type, clay cation exchange capacity (CEC), sodium-saturated and TAT-saturated d(001) spacings, and the change in d(001) spacing with TAT saturation for the <1 µm size fraction of the seven smectites used in this study.
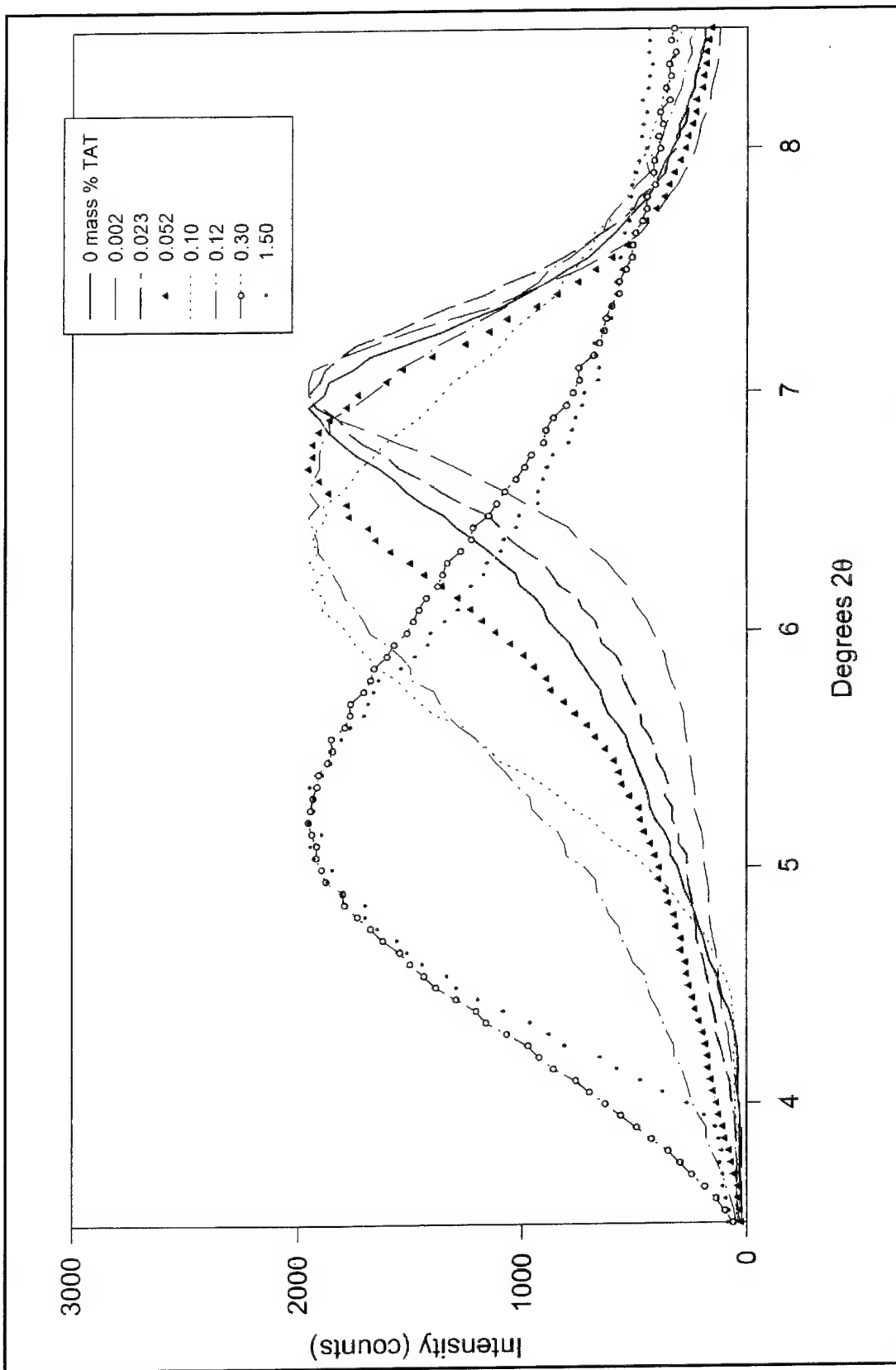
Figure 3.   Superimposed STx-1 diffraction patterns showing peak movement with TAT loading
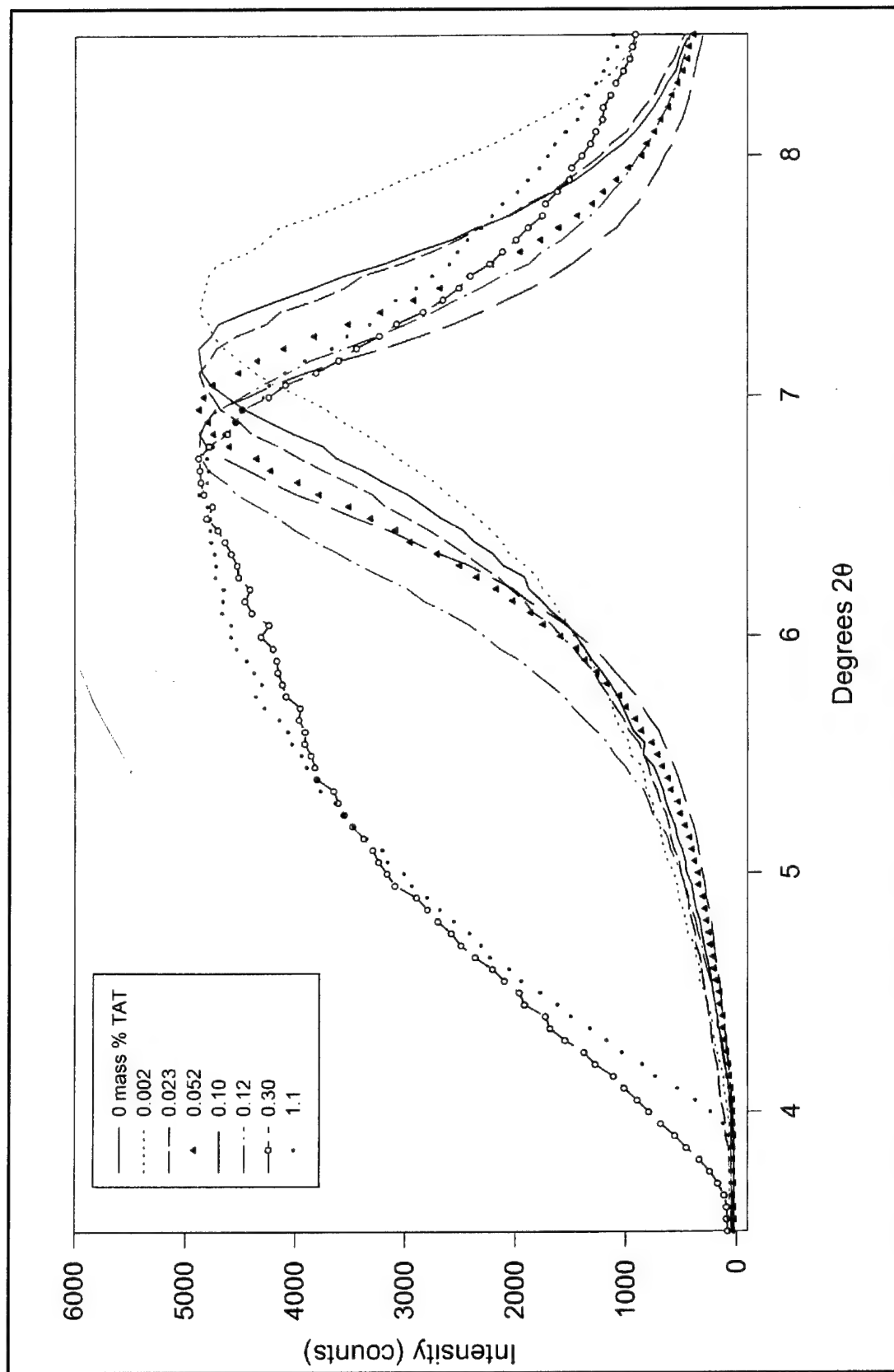
Figure 4. Superimposed SWy-1 diffraction patterns showing peak movement with TAT loading
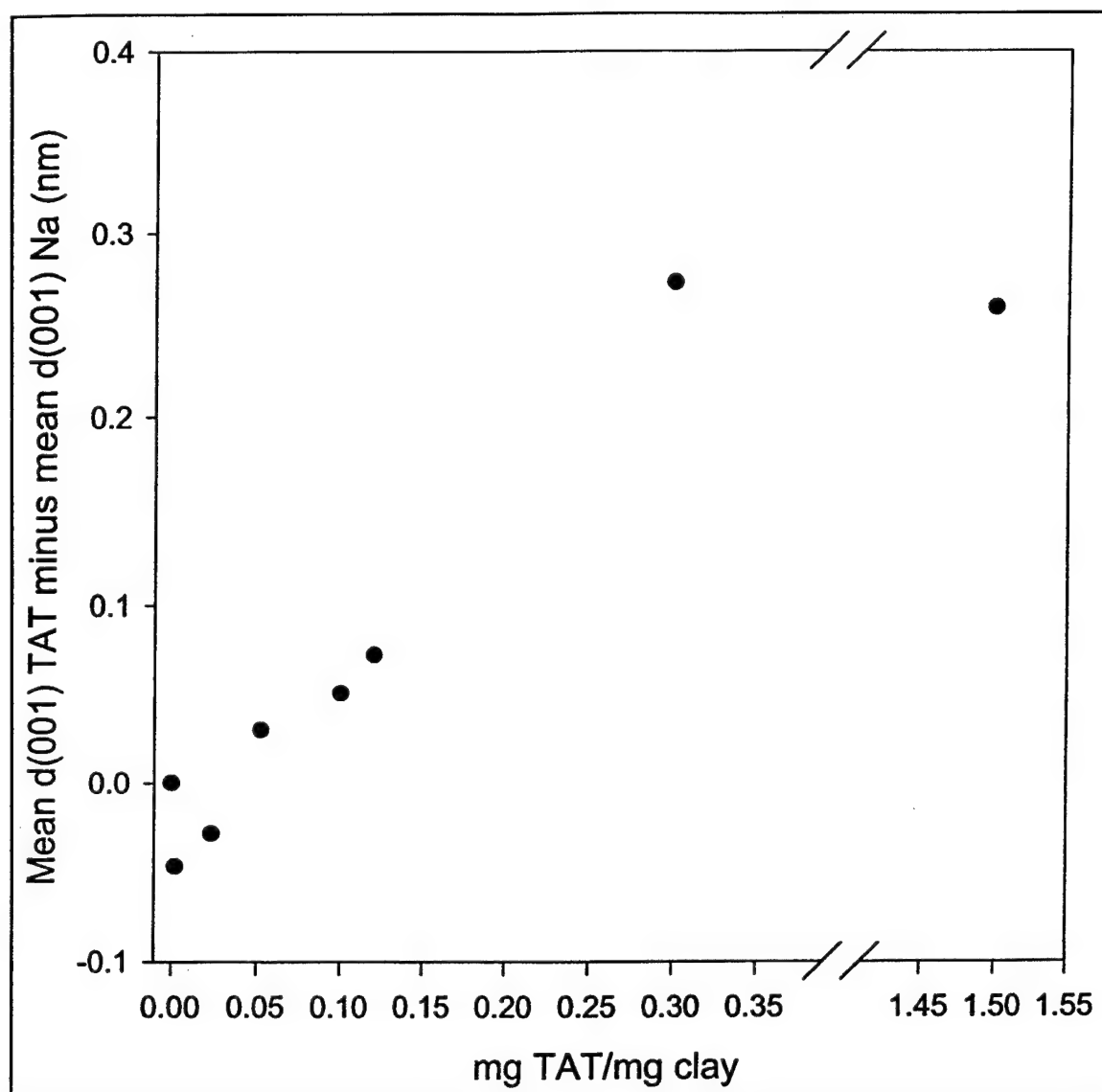
Figure 5. TAT loading vs change in the mean d(001) peak position for STx-1

Three cation loadings were used to obtain XRD patterns for each clay type: sodium-saturated homoionic clay, partially loaded with TAT 0.48 mg TAT/40 mg clay-intermediate loading (12 mass percent), and saturated with TAT (saturated). Figures 7-13 contain XRD patterns for each clay. For each figure, the top panel displays the three unscaled diffraction patterns for sodium-saturated, 12 mass percent, and saturated. The middle panel presents the same data scaled such that the maximum intensity at the d(001) peak is the same for the sodium-saturated, 12 mass percent, and saturated patterns. In the bottom panel, the patterns are once again scaled such that the maximum intensity of the d(001) peak is the same for the sodium-saturated, intermediate TAT, and saturated TAT loading patterns, and the x-axis is limited to the region in which the d(001) peak occurs. The XRD patterns displayed in Figures 7-13 show the shift in the peak associated with reflections from the d(001) spacing (between 4 and 9° 2θ) as the TAT loading is increased.
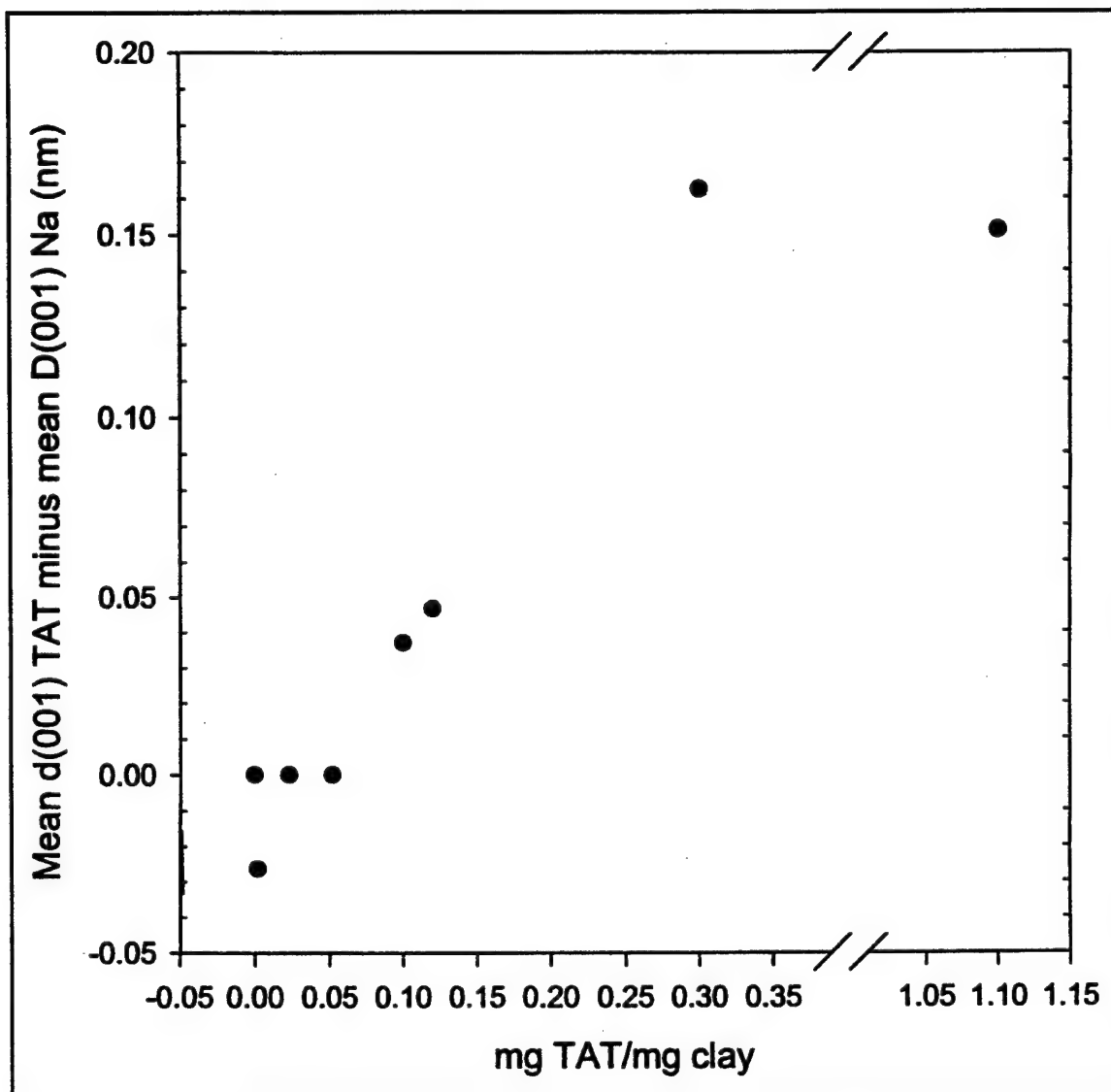
Figure 6.   TAT loading vs change in the mean d(001) peak position for SWy-1

In order to compare the expansions of the seven smectites used in this study, the d(001) peaks are presented in Figures 14-16 for the seven clay types under the three loading conditions. Figure 14 displays the sodium-saturated peaks for all seven smectites. The peak position is between 1.23 and 1.28 nm which corresponds to a single water layer surrounding sodium cations in the interlamellar region. Figure 15 shows the same seven clays loaded at 12 mass percent. Differences between the d(001) spacing in the seven clays from those in Figure 14 display a trend from smallest to largest expansion following the order SBF-1, SWa-1 < SWy-1, STx-1 < SapCa-1 < SHCa-1 < SAz-1. Two clays, SHCa-1 and SAz-1, expanded the most (1.42 and 1.46 nm) under the same loading conditions. The extent of shifting of the d(001) peak, as well as the peak shape, is similar for the rest of the samples.

Table 4
Variation of TAT Adsorption in Clay Samples

Sample	CEC, meq/100g	mean d(001) of Na-saturated clay, nm	mean d(001) of 12 mass % loaded clay, nm	mean d(001) of 12 mass % minus mean d(001) of Na-saturated clay, nm	mean d(001) of TAT-saturated clay, nm	mean d(001) of TAT-saturated minus mean d(001) of Na-saturated clay, nm
SBF-1[1]	85.0	1.262	1.318	0.056	1.338	0.076
STx-1[2]	88.3	1.308	1.391	0.083	1.563	0.255
SAz-1[2]	130.0	1.244	1.424	0.180	1.549	0.305
SHCa-1[2]	89.2	1.262	1.402	0.140	1.509	0.247
SapCa-1[2]	80.4	1.253	1.448	0.195	1.460	0.207
SWy-1[2]	87.0	1.262	1.308	0.046	1.402	0.140
SWa-1[2]	107.0	1.271	1.318	0.047	1.460	0.189

[1] CEC data from Low (1980)
[2] CEC data from Jaynes and Bigham (1987)

Figure 16 shows the same seven clays at the final or saturated loading of TAT. These clays were treated with an excess amount of 300 ppm TAT-(HCl)$_3$ solution. At this point all clays had been allowed to adsorb TAT following the experimental loading conditions until the clays did not remove appreciable amounts of TAT from the aqueous solution. At this loading level, the differences between the d(001) spacing in the seven clays are more significant than observed in Figure 15. The peaks in Figure 16 appear to be a composition of two peaks, one centered around the 1.30 nm range and one centered around 1.77 nm. The mean d(001) peak position follows a trend of SBF-1 < SWy-1 < SapCa-1 < SWa-1 < SHCa-1, STx-1 < SAz-1. The asymmetric peak shape can be explained by the presence of a range of d(001) spacings in these clays, dominated by the two separations at 1.30 and 1.77 nm.

It is interesting to compare the maximum spacing between layers of the TAT-saturated clays with the CEC. Figure 17 shows a plot of clay CEC versus the weighted d(001) spacing at 12 mass percent TAT loading and TAT saturation. A roughly linear relationship is observed with exceptions including STx-1, SBF-1, and SHCa-1 indicating that CEC is not the only clay property that governs the maximum increase in d(001) spacing possible by TAT adsorption. It also is interesting to note that for the intermediate and maximum loading of TAT for this series of smectites, both the trioctahedral clays SapCa-1 and SHCa-1 show increased expansion of the interlayer compared to all of the other clays except for STx-1. This observation that the trioctahedral clays expand more than dioctahedral clays with similar CECs may relate to the structural and chemical differences between trioctahedral and dioctahedral smectites which have been
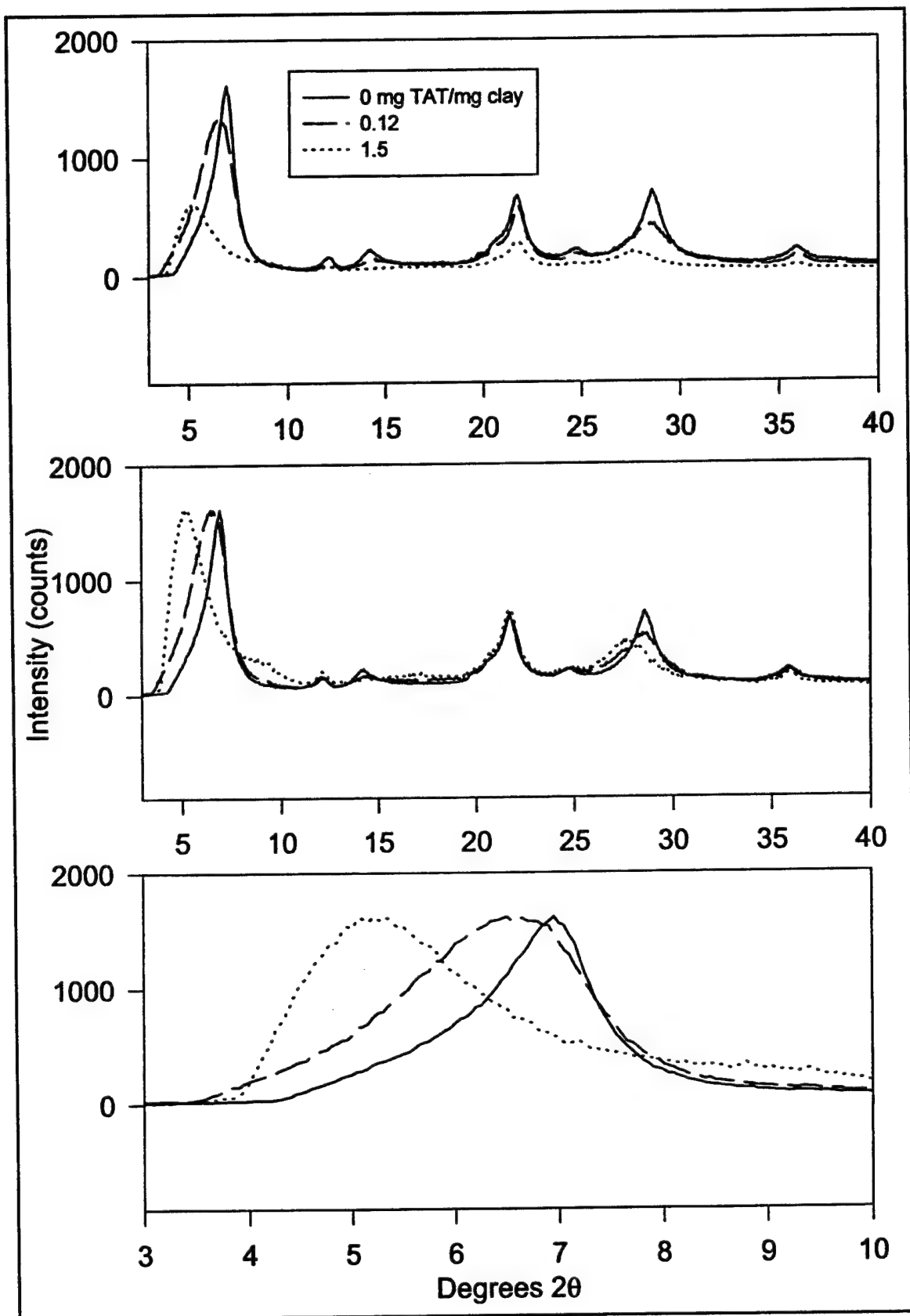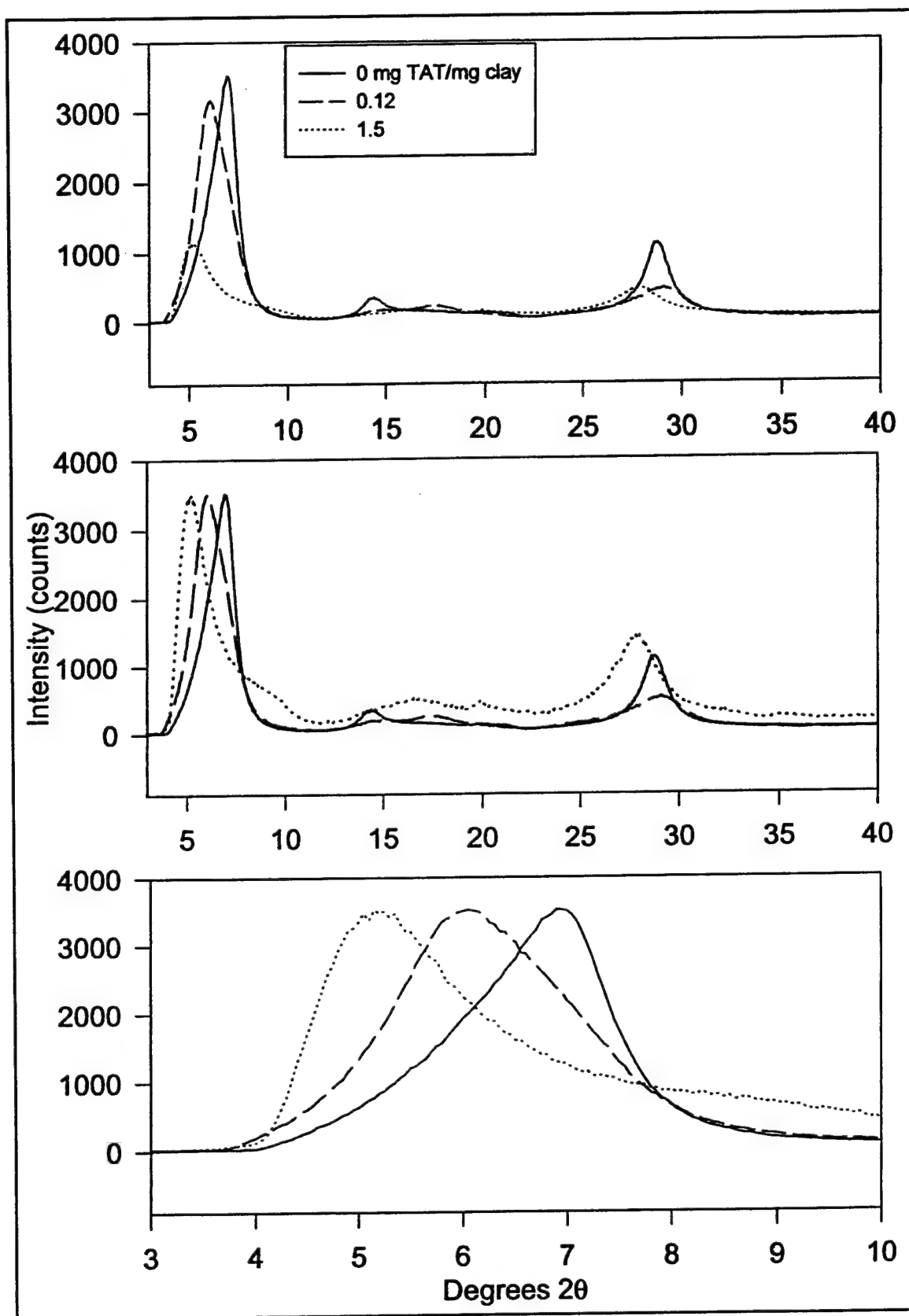
Figure 7.   XRD pattern for STx-1

Figure 8.   XRD pattern for SAz-1

Figure 9.   XRD pattern for SBF-1
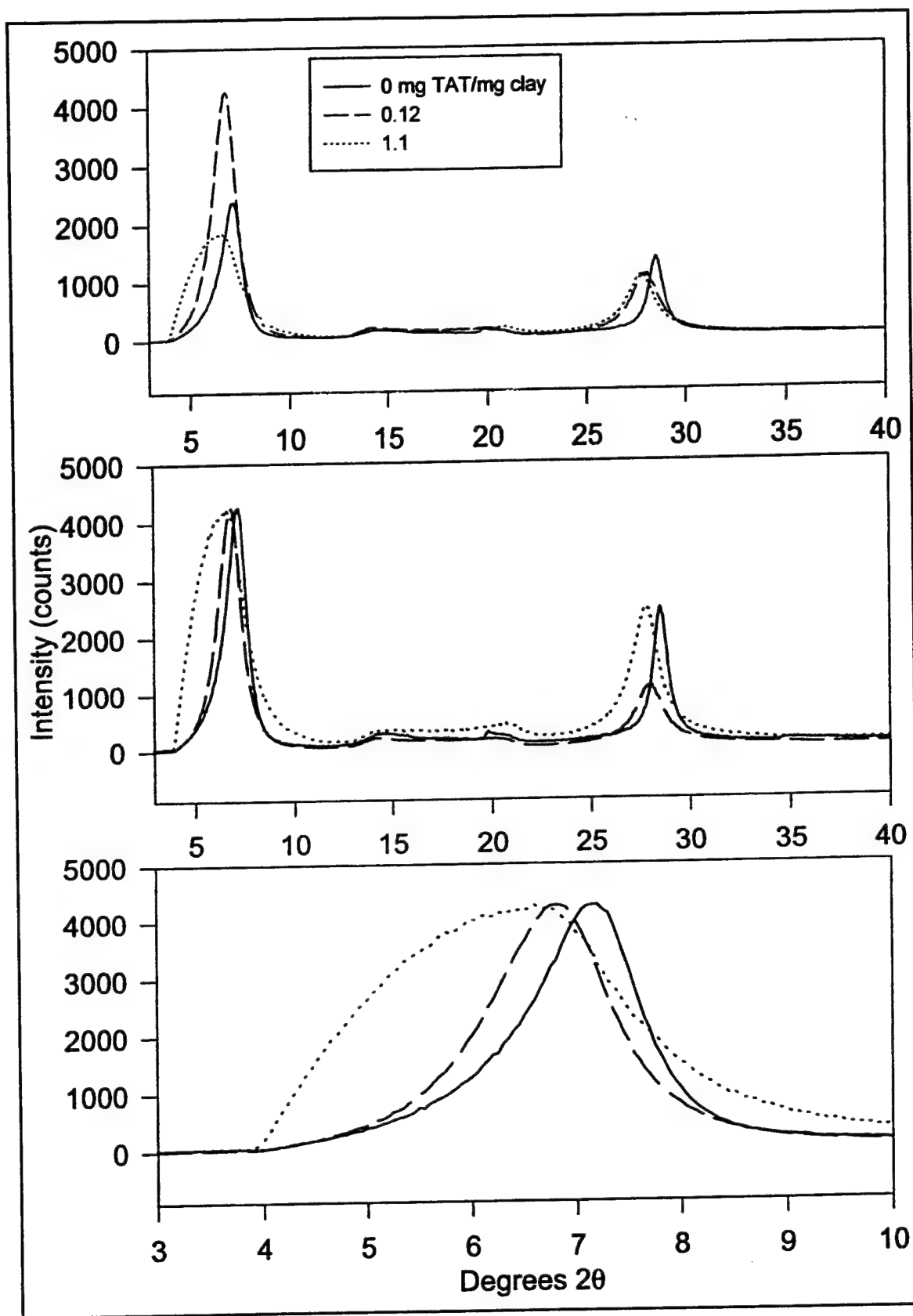
Figure 10.   XRD pattern for SWy-1
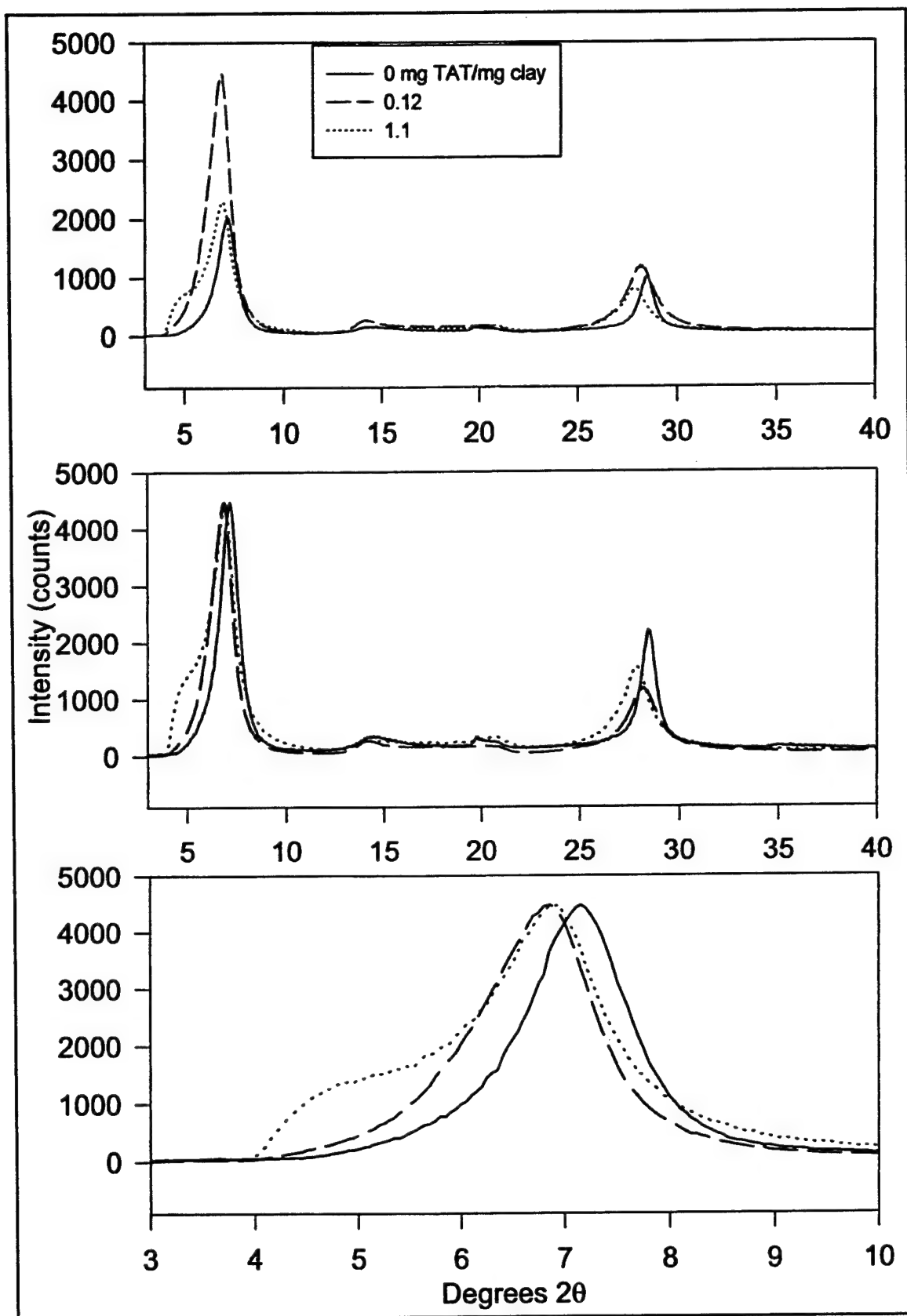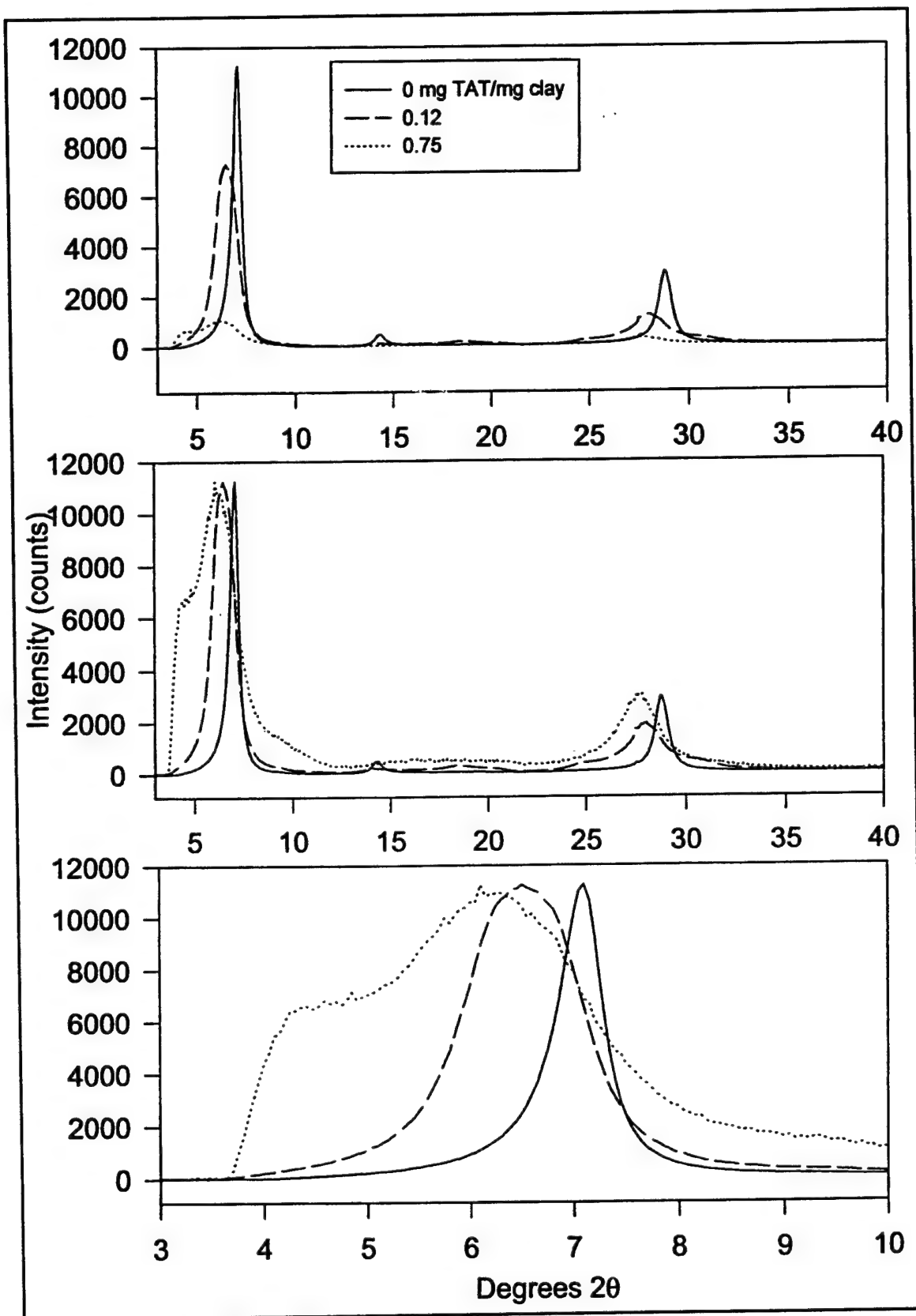
Figure 11. XRD pattern for SapCa-1

Figure 12. XRD pattern for SHCa-1
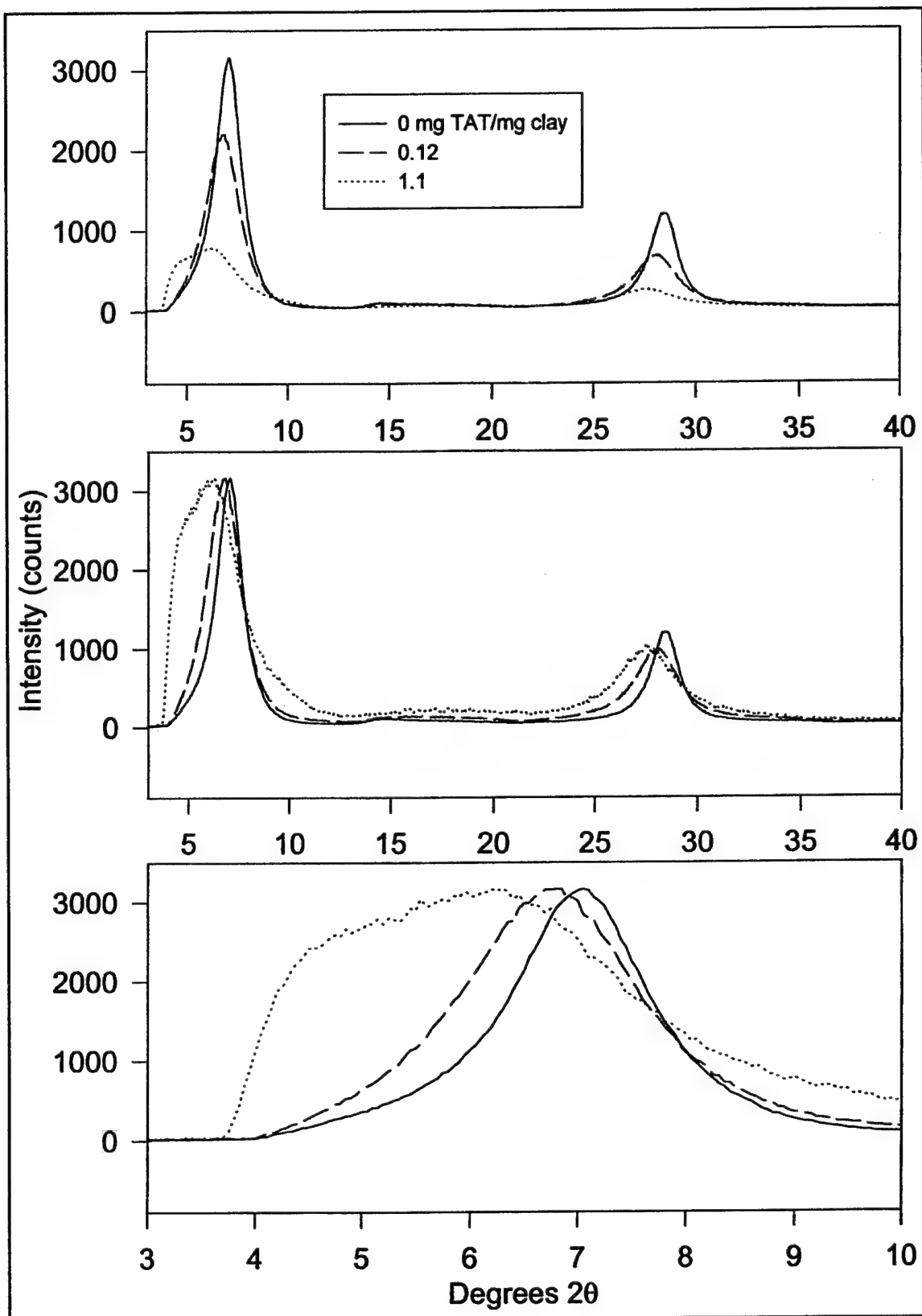
Figure 13. XRD pattern for SWa-1
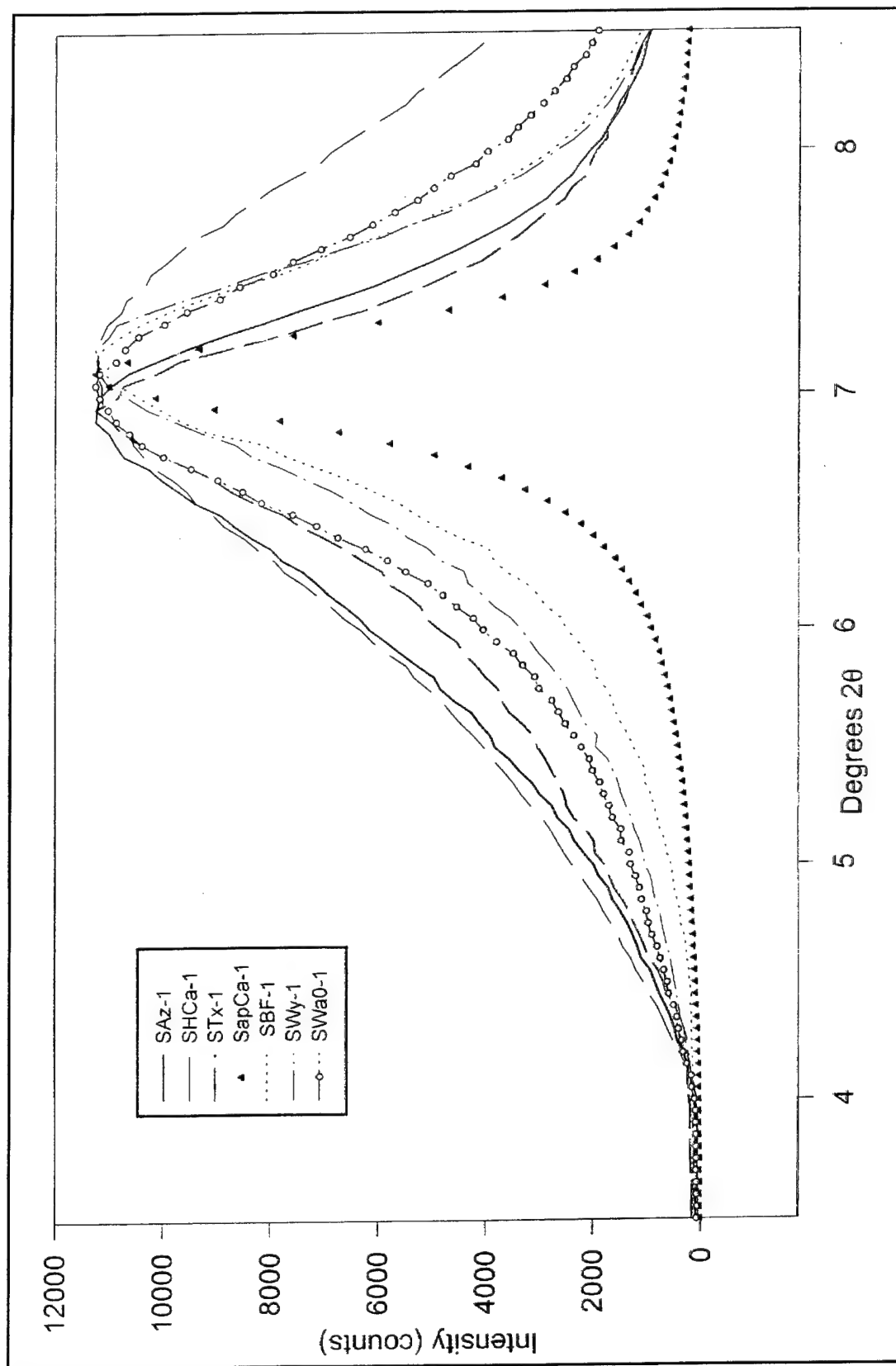
Figure 14. XRD, d(001) peaks for sodium-saturated smectites

Legend:
- SAz-1
- SHCa-1
- STx-1
- SapCa-1
- SBF-1
- SWy-1
- SWa0-1

Intensity (counts)

Degrees 2θ

Figure 15.   Twelve mass percent TAT d(001) peak for smectites

Figure 16. TAT-saturated d(001) peaks for smectites

Figure 17.   CEC vs increase in mean d(001) peak position for smectites examined

shown to affect the clay structure, as well as the chemistry of the interlayer as indicated by Si-29 and Cs-133 nuclear magnetic resonance (NMR) spectroscopy as shown by Weiss, Kirkpatrick, and Altaner (1990a, b) and Weiss, Altaner, and Kirkpatrick (1987). Also the location of the layer charge (tetrahedrally o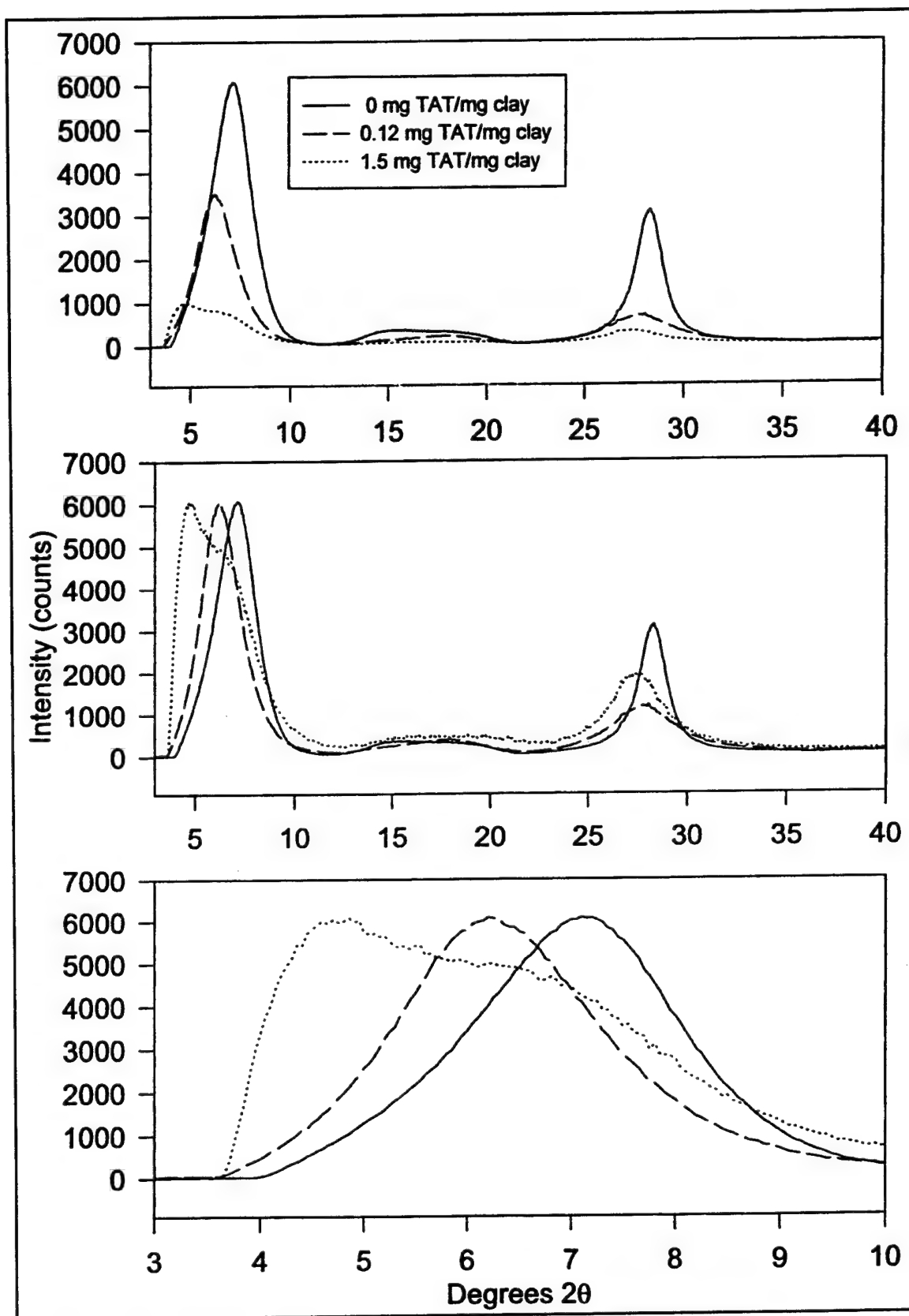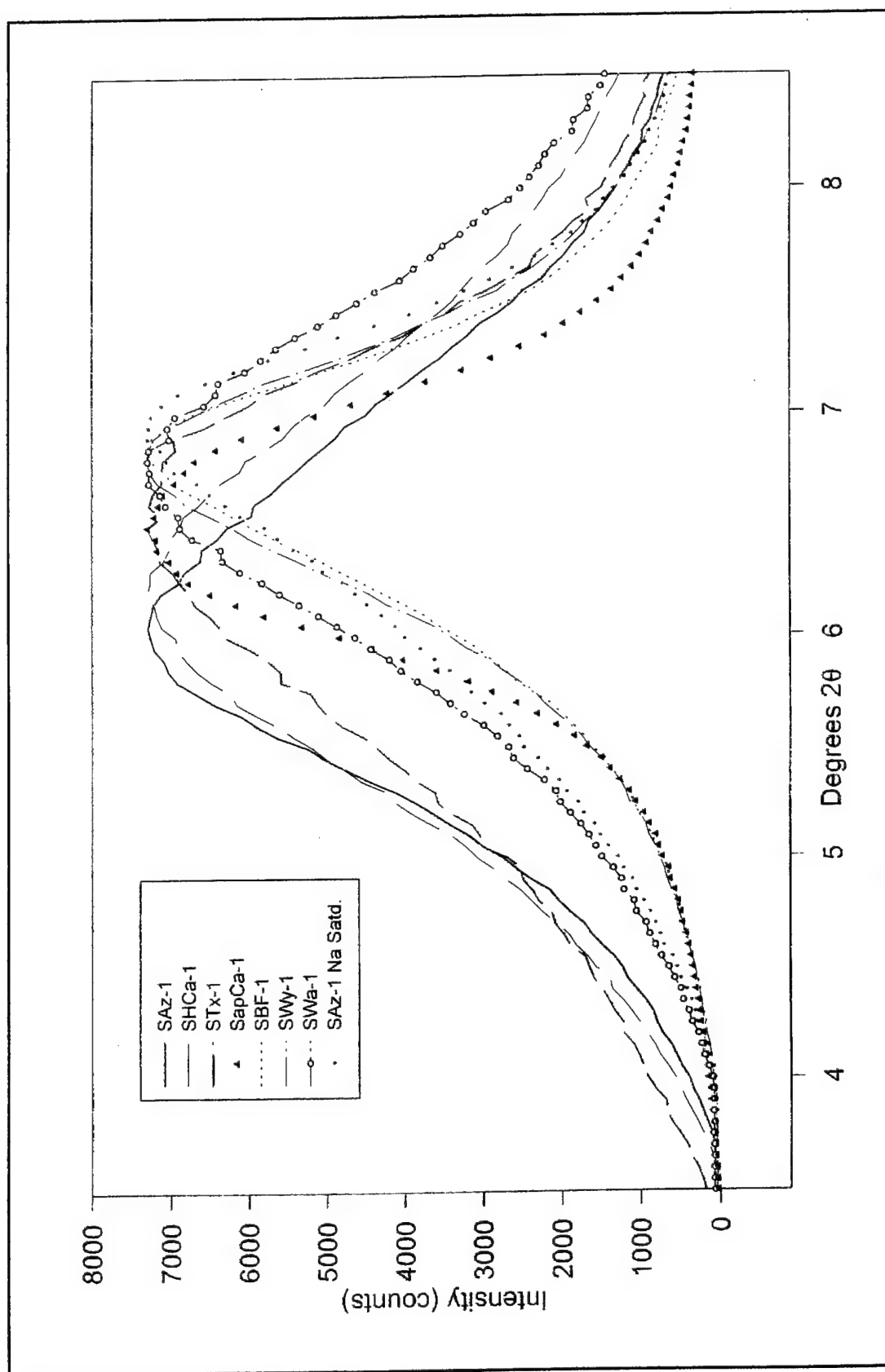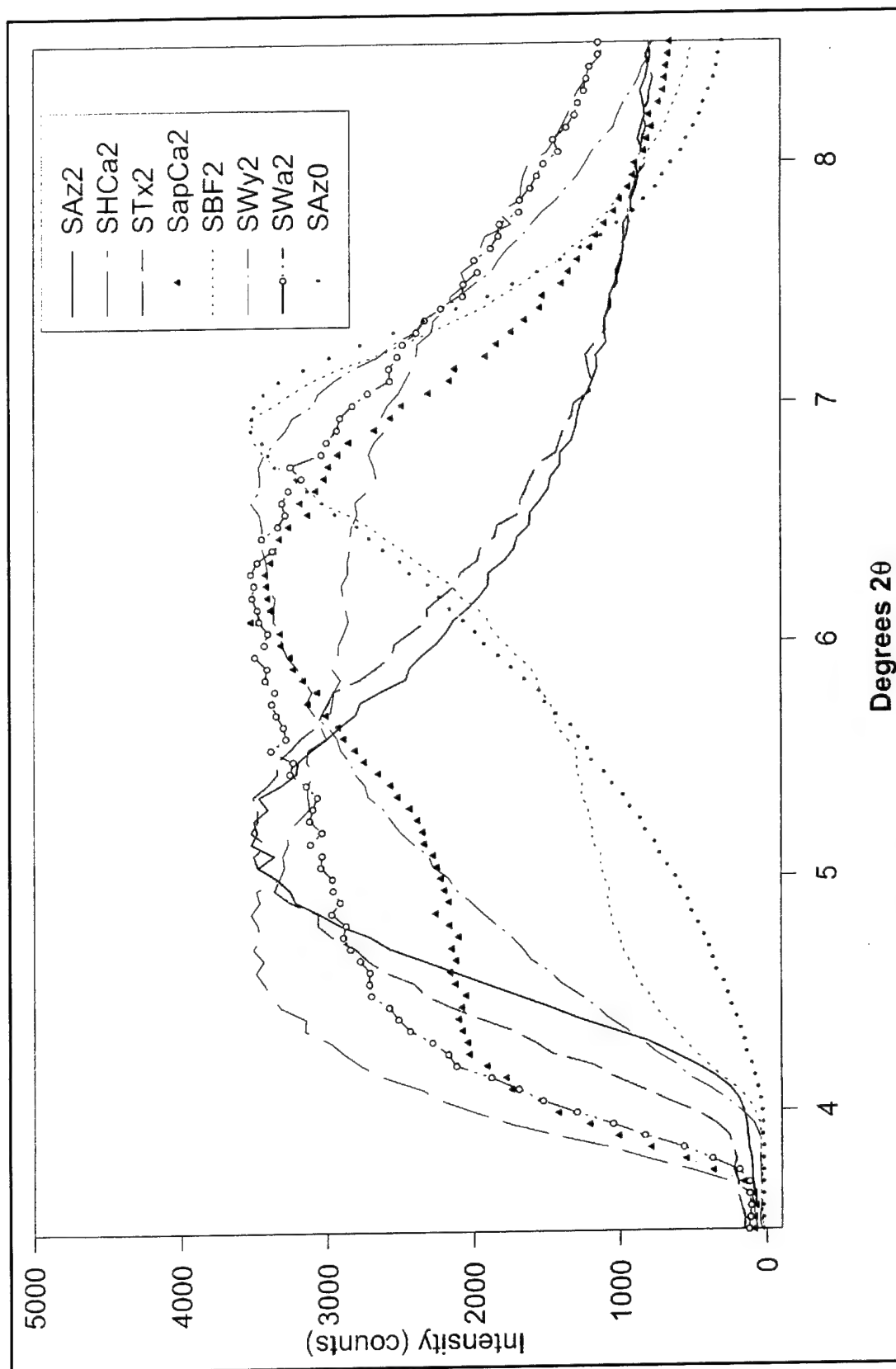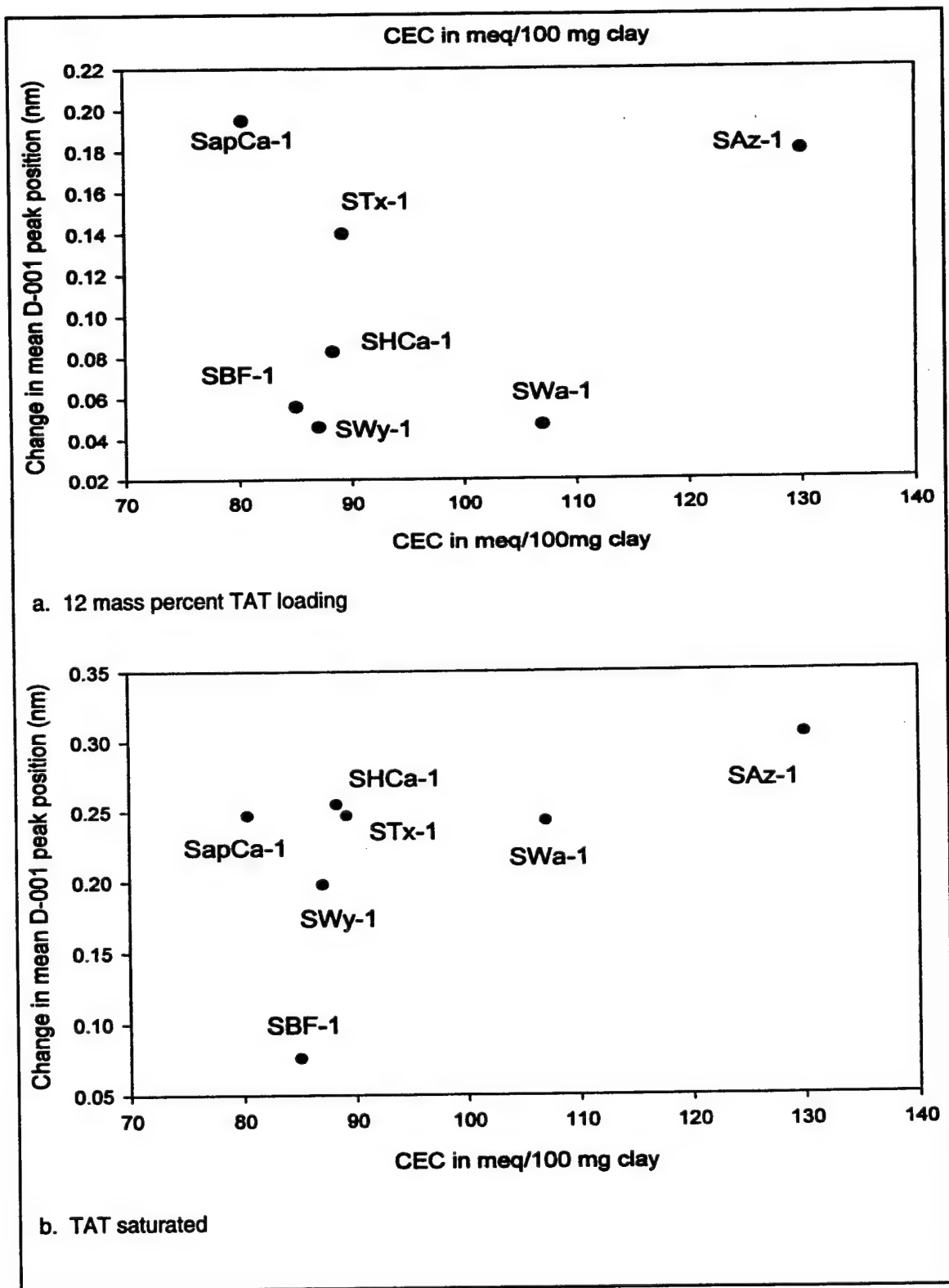r octahedrally derived) may influence the adsorption of TAT on clays because (a) the location of the layer charge is closer to the interlayer for clays with tetrahedrally derived layer charge, and (b) the charge distribution for trioctahedral clays may be more uniform with 3 Mg atoms compared to dioctahedral clays with 2 Al atoms and one vacancy. This cannot be assessed, as only one smectite with tetrahedrally derived layer charge (SapCa-1) was examined in this study. Additional samples, such as beidellites or other saponites, may assist in these interpretations.

Mechanism of TAT Loading in the Interlayer of Expandable Clays

The patterns displayed in Figures 7-16 provide a basis for discussion of the adsorption mechanism. Because all of the clays were treated with the same amount of TAT during the intermediate loading (Figure 15), one would expect that if the TAT were cation exchanging in a uniform pattern on all clays, a range of d(001) spacings similar to that observed for the sodium-exchanged clays for the seven clays would be expected. The large variation of d(001) spacing within this series is possibly a result of the trifunctional anionic character of the TAT molecule. The spatial separation of the three monocationic sites on the molecule by the rigid phenyl ring allows a number of loading geometries for cation exchange adsorption. If one, two, or all three cationic sites of a given TAT molecule are associated with both of the aluminosilicate sheets above and below the molecule, such that the TAT molecule can lie in a flat position between the two sheets, then the d(001) spacing would correspond to the increased height of the hydrated TAT cation lying in the plane of the sheets. This height is expected to be comparable to the spacing observed when ammonium cation is present in the interlayer of clays. The effect of ammonium (NH_4^+) on the basal spacing of hydrated Wyoming montmorillonite is reported to be 1.24 nm (MacEwan and Wilson 1980). Comparing this basal spacing to that of a sodium-exchanged Wyoming montmorillonite would predict a decrease in d(001) spacings when TAT takes on this geometry. This initial decrease in d(001) spacing is observed with STx-1 and SWy-1 at low TAT loadings in Figures 3 and 4.

The TAT molecule can occupy a larger amount of the interlayer space by having one cationic functionality associated with one 2:1 layer and another cationic site on the same molecule associated with the other 2:1 layer. If this occurs, then the rigid phenyl ring of the TAT molecule could act as a spacer, forcing the interlamellar distance farther apart. By adsorbing in a vertical or "standing" position in this way, the d(001) spacings can become increasingly large, with a maximum separation corresponding to the distance between the two hydrated, cationic sites.

Higher Order Stacking of Clay Layers Under TAT Loading

The higher order stacking uniformity can be determined from the XRD patterns for the seven clays at the three TAT loading levels. The ratio of the higher order reflections (HOR) observed between 25 and 30 °2θ to the d(001) peak indicates the degree of high order stacking. These peaks can be seen in Figures 7-13. This ratio provides information regarding the higher order structure of the stacked clay structures. The higher order reflection intensity depends on the repeatability of single layer stacking. A high ratio would indicate an ordered, layered system while a low ratio would indicate a lack of homogeneous layer stacking. The measurement of d(001) distances is possible for clays without highly ordered and repeatable units because only the reflections from a single layer are required. The intensity of the higher order reflections, however, depends on the uniformity of the interlayer distances. For the sodium-exchanged clays, a high level of stacking order is observed as a result of the uniform layering associated with this hard, monocationic species within the clay. The ratio of higher order reflection to d(001) intensity as TAT is loaded into the clay provides information regarding the mechanism of cation exchange. Table 5 presents the ratio of HOR to d(001) for the seven clays at the three loading levels examined.

Table 5 HOR:d(001) for Sample Clays				
		HOR:d(001) peak intensity		
Sample	CEC, meq/100g	Na saturated	12 mass percent	TAT saturated
SBF-1	85	0.49	0.27	0.35
STx-1	88.3	0.44	0.32	0.32
SAz-1	130	0.32	0.15	0.42
SHCa-1	89.2	0.52	0.2	0.33
SapCa-1	80.4	0.27	0.17	0.29
SWy-1	87	0.58	0.26	0.58
SWa-1	107	0.38	0.31	0.34

For all seven clays the ratio of HOR to d(001) is high for the completely sodium-exchanged sample. This is understandable because the hard, monocationic form of sodium produces a highly homogeneous stacking. When the intermediate level of TAT is placed on the seven clays, the ratio of HOR to d(001) decreases in all of the clays. This decrease is expected due to the incomplete replacement of the sodium cations by the TAT molecules. This incomplete replacement results in heterocationic clay. For the seven clay types, all of the TAT-saturated clay samples show an increase, except STx-1 which shows a slight decrease, in the ratio of HOR to d(001) compared to the incomplete loading. This would be expected as more of the sodium cations are replaced by the TAT cations and the d(001) spacings become more uniform for a

high CEC clay like SAz-1 in which the intercalating cation obtains a uniform orientation.

The changes in the ratio of HOR to d(001) spacings observed in Table 5 can be explained using a simplified model of the mechanism for TAT adsorption. Figure 18 shows a representation of a completely sodium-exchanged stacking of clay layers. The red areas are the aluminosilicate clay layers, and the blue areas represent the hydrated sodium occupying the interlamellar regions. The d(001) spacing is 1.25 nm and the stacking of four of these repeating units results in the HOR. Because of the completeness of the exchange and the uniformity of interlamellar adsorption of the spherical, monovalent cation, the d(001) spacing is uniform and a high ratio of HOR to d(001) is observed. As TAT is initially adsorbed onto the clay, the repeatability of the d(001) units is reduced. This is illustrated in Figure 19. The green areas represent the larger TAT cations adsorbed to the interlayer. The combination of sodium (blue) and TAT (green) cations within the interlayer results in a loss of d(001) spacing uniformity. This loss of uniformity results in the loss of higher ordered stacking which provides the d(001) reflection. Using this model, the reduction in the ratio of the HOR to d(001) intensities for the intermediate loading shown in Table 5 can be explained. For these "edge loaded" clays (with > 5 mass percent TAT) an increase in the d(001) spacing is observed, but with a decrease in peak intensity of the d(001) peak due to the range of d(001) spacings possible. Furthermore, a loss of the higher order peak intensities results from the loss of higher order stack uniformity. When the clay becomes saturated with TAT, a uniform distribution of the TAT cation throughout the interlayer surface results. Figure 20 displays a representation of this situation. Because the clay has adsorbed all the TAT possible, the d(001) spacing is more uniform throughout the sample and the intensity of the HOR begins to return.

Effect of TAT Loading on FTIR Spectrometry of Clays

In order to further understand the chemical transformation occurring during the loading of TAT in the interlayer of expandable clays, FTIR spectroscopy of a set of pure clays and TAT-(HCl)$_3$ as well as two mixtures of TAT and clay was performed. Three clay preparations were utilized for this investigation: sodium-exchanged STx-1, STx-1 saturated with TAT by adsorption in an aqueous suspension, and a physical mixture prepared by grinding dry STx-1 and dry TAT-(HCl)$_3$ using a mortar and pestle. The ratio of mass of TAT to mass of clay in the two STx-1/TAT-(HCl)$_3$ samples is approximately the same (within 10 percent). The infrared (IR) spectrum of pure TAT-(HCl)$_3$ was also obtained. Figure 21 displays the IR spectra of the three clay samples in the wavelength range from 500 to 4,000 nm. The spectrum of sodium-exchanged STx-1 (Figure 21, i) and the TAT-saturated STx-1 (Figure 21, iii) appear to be quite similar in adsorption amplitude and energy. Increased adsorbance in the TAT-saturated sample
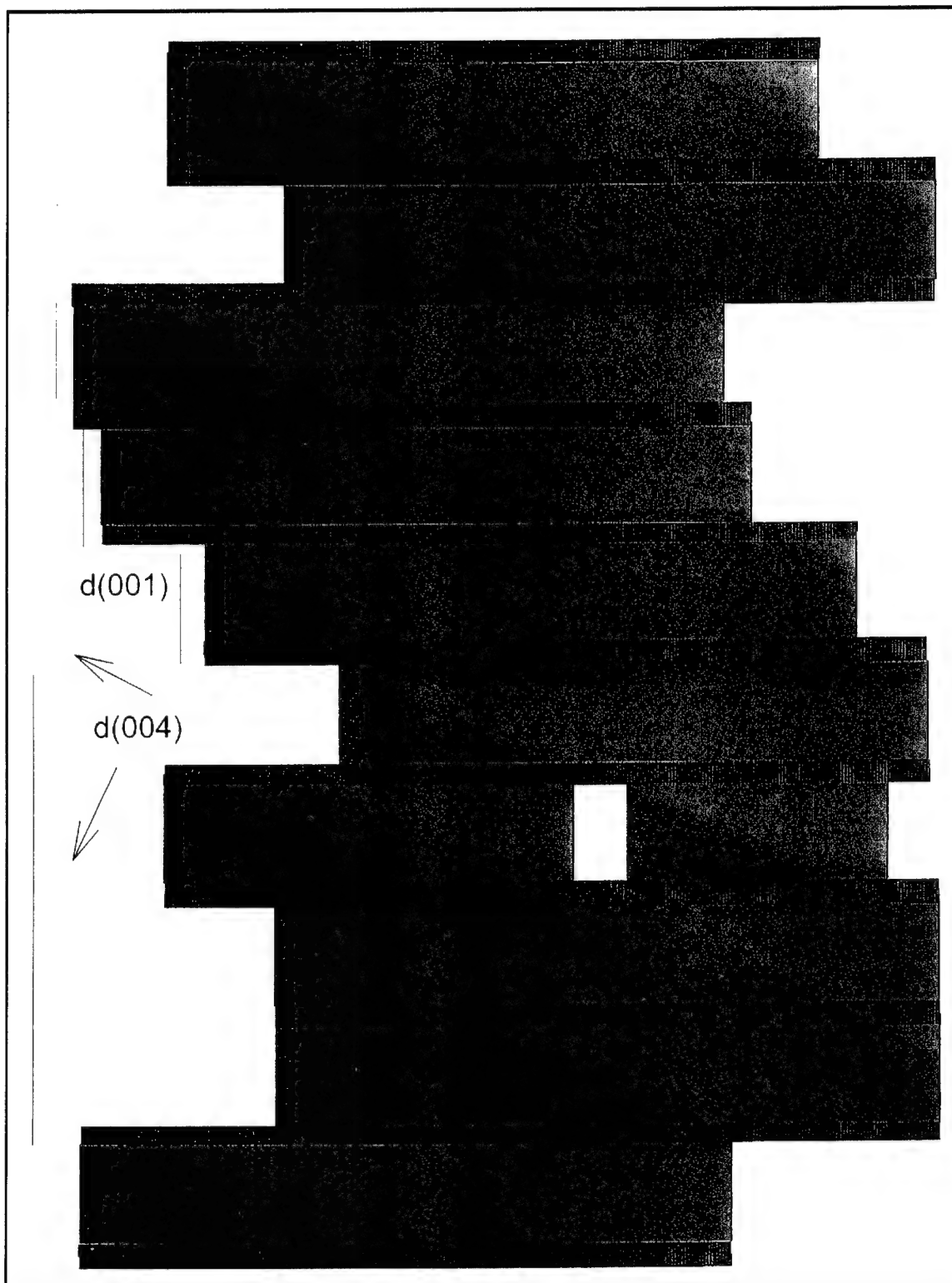
d(001)

d(004)

Figure 18. Homogeneous loading of sodium on clay showing higher order symmetry
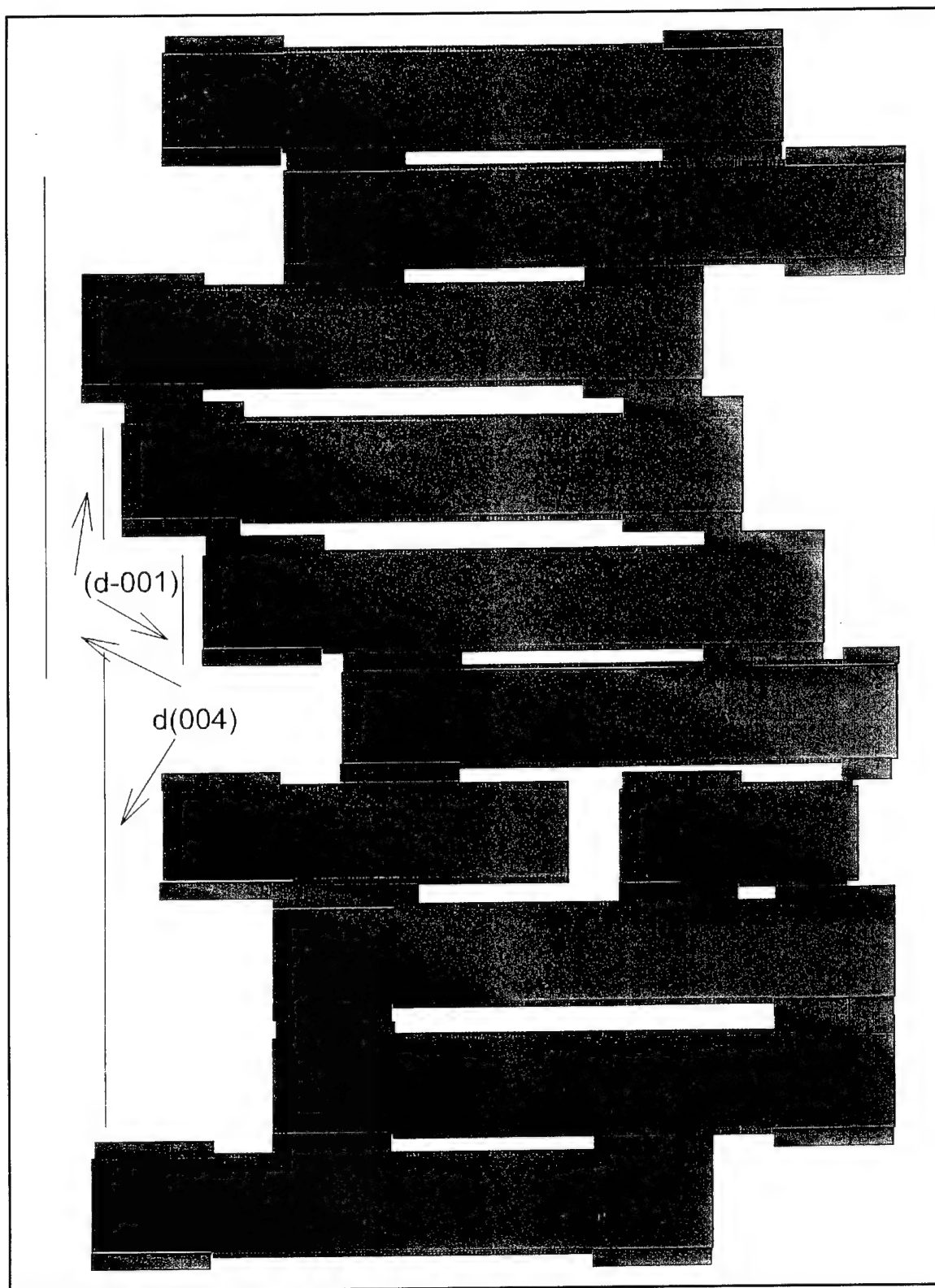
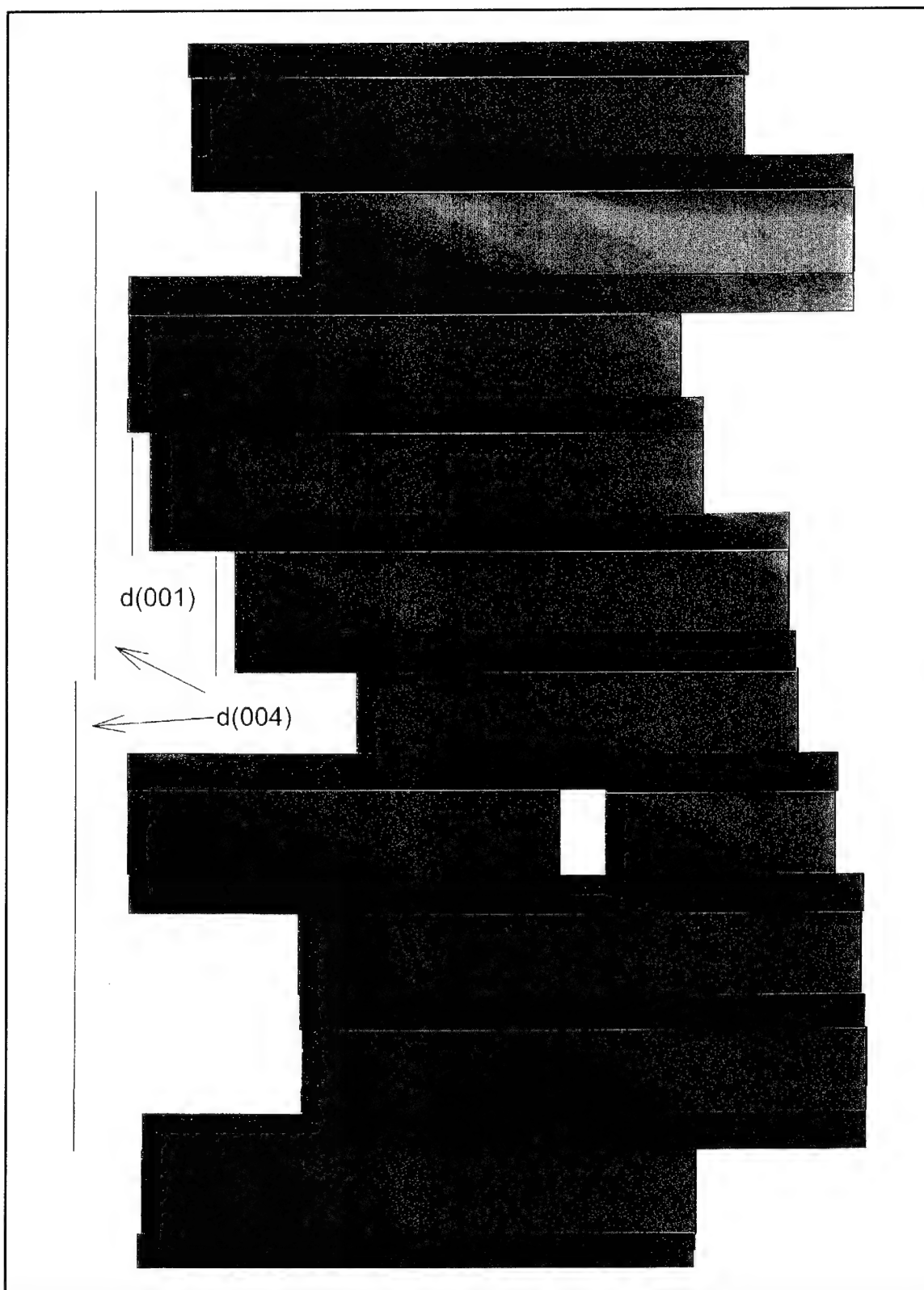Figure 19. Edge loading of TAT on clay showing loss of higher order symmetry

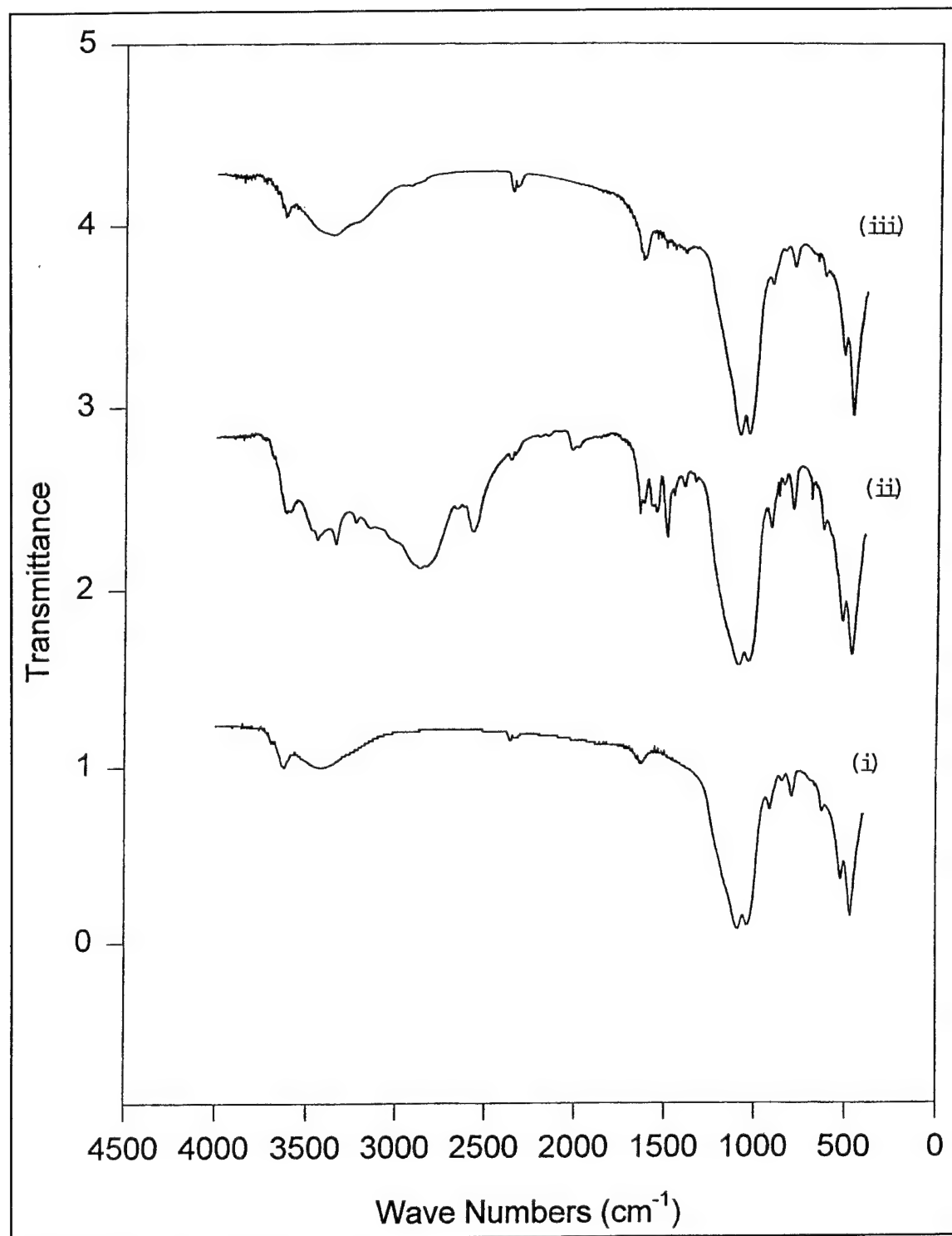Figure 20. Homogeneous loading of TAT on clay showing increased higher order symmetry

Figure 21. Infrared spectra of the three clay samples: (i) STx-1, (ii) physical mixture of STx-1 and TAT, and (iii) TAT adsorbed on STx-1

appears between 3,600 and 3,000 nm and between 2,000 and 1,500 nm. The increased adsorption in these two wavelength regions appears to be a result of molecular vibrations associated with the sorbed organo-cations produced during the clay catalyzed transformation of the TAT polycation. The physical mixture of TAT and STx-1 (Figure 21, ii) displays increased adsorption of IR energy in the 4,200 and 2,500 nm and between 2,000 and 400 nm regions. This spectrum is significantly different than that of the pure clay or TAT sorption samples.

In order to visualize the differences in the IR spectrum of the pure clay and the spectra of the two mixtures, a subtraction of the scaled spectra of either pure compound (STx-1 or TAT-(HCl)$_3$) from the spectra of the two mixtures was performed. These two artificially produced spectra are displayed in Figures 22 and 23 along with the spectrum of the pure compound that was not removed by spectral subtraction.

Figure 22 displays the IR spectrum of TAT-(HCl)$_3$ (curve i), the spectrum obtained by subtracting the IR spectrum of STx-1 from the IR spectrum of the TAT/STx-1 mixture (curve ii), and the spectrum obtained by subtracting the IR spectrum of STx-1 from TAT-saturated STx-1 (curve iii). Very little difference is observed when the TAT spectrum is compared to the dry TAT/STx-1 mixture minus the STx-1 spectrum. The similarity between the IR spectrum of TAT and that obtained by subtracting that of the pure STx-1 from the TAT/STx-1 mixture suggests that no significant interactions or reactions are occurring when the dry STx-1 and the TAT-(HCl)$_3$ solid are mixed.

All of the spectral features are present at the same wavelengths, and the intensities of the adsorptions are comparable. A comparison of the TAT spectrum with the spectrum obtained by subtracting the STx-1 spectrum from that obtained from the TAT-saturated STx-1 shows significant differences. The adsorbance observed in the spectrum of pure TAT in the region from 2,250 to 3,250 nm is not present in the subtracted spectrum. While there appears to be significant adsorbance in the regions from 1,400 to 1,700 nm and 4,000 to 3,400 nm in the spectrum prepared by subtracting the STx-1 spectrum from the TAT-saturated STx-1, the position of these peaks does not correspond to those in the pure TAT spectrum. An interesting feature of Figure 22 curve iii is the apparent negative adsorbance observed near 3,700 cm^{-1}. The peak in this region in the spectrum of pure clay represents the adsorption of IR radiation by the hydroxide functionalities of the clay mineral. This feature is clearly seen in the spectra of pure STx-1 in Figure 21, curve i. The negative peak observed during subtraction suggests that the adsorption of IR radiation by these functionalities is altered by the presence of adsorbed TAT or TAT transformation products. The differences noted between the IR spectrum of TAT and that obtained by subtracting that of the pure STx-1 from the TAT-saturated STx-1, however, suggest that intercalation of the TAT cations or clay catalyzed transformations of the TAT cations are occurring when the STx-1 and the TAT in solution are mixed.
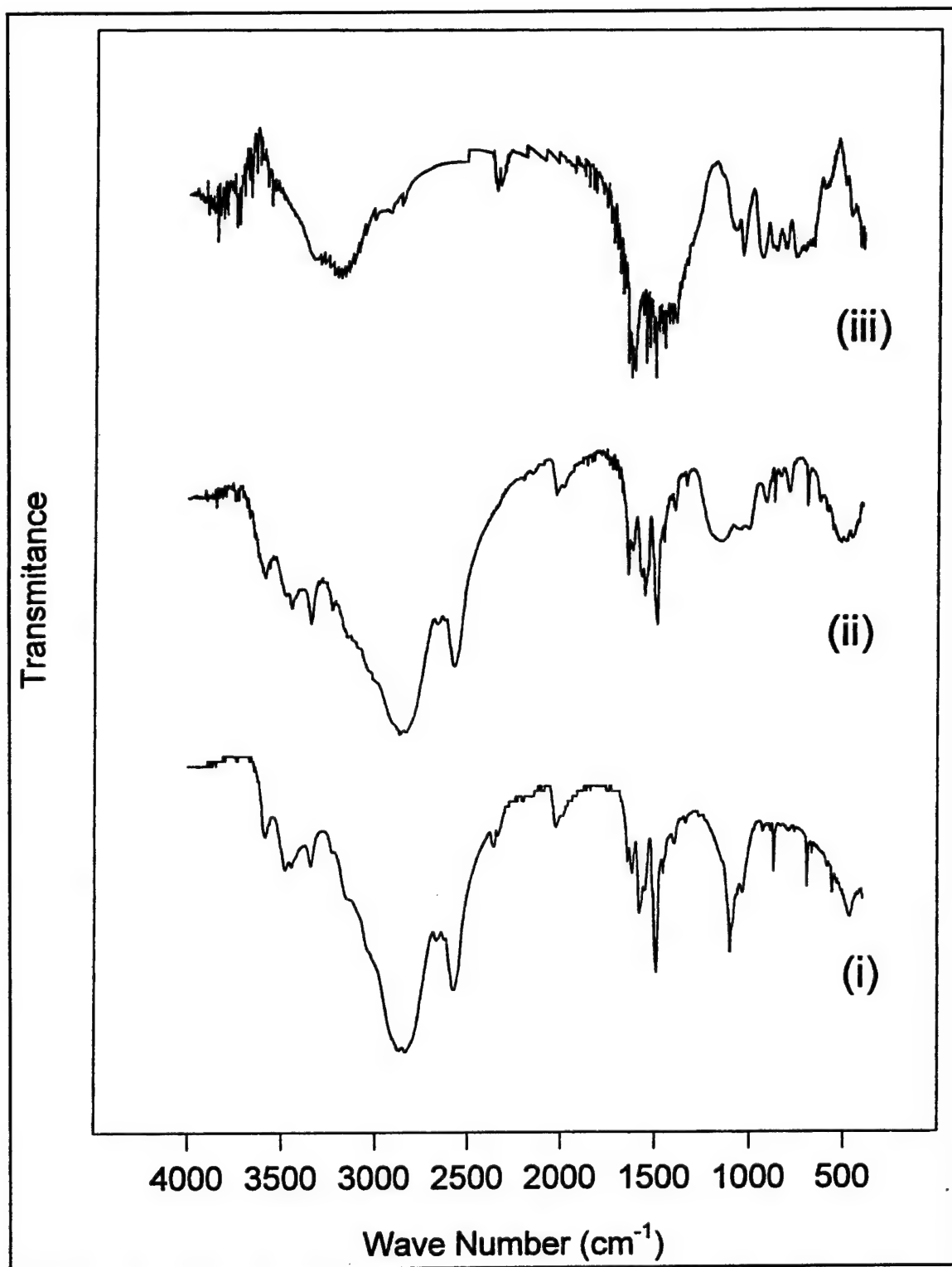
Figure 22. Infrared spectra: (i) TAT, (ii) physical mixture of STx-1 and TAT minus the scaled
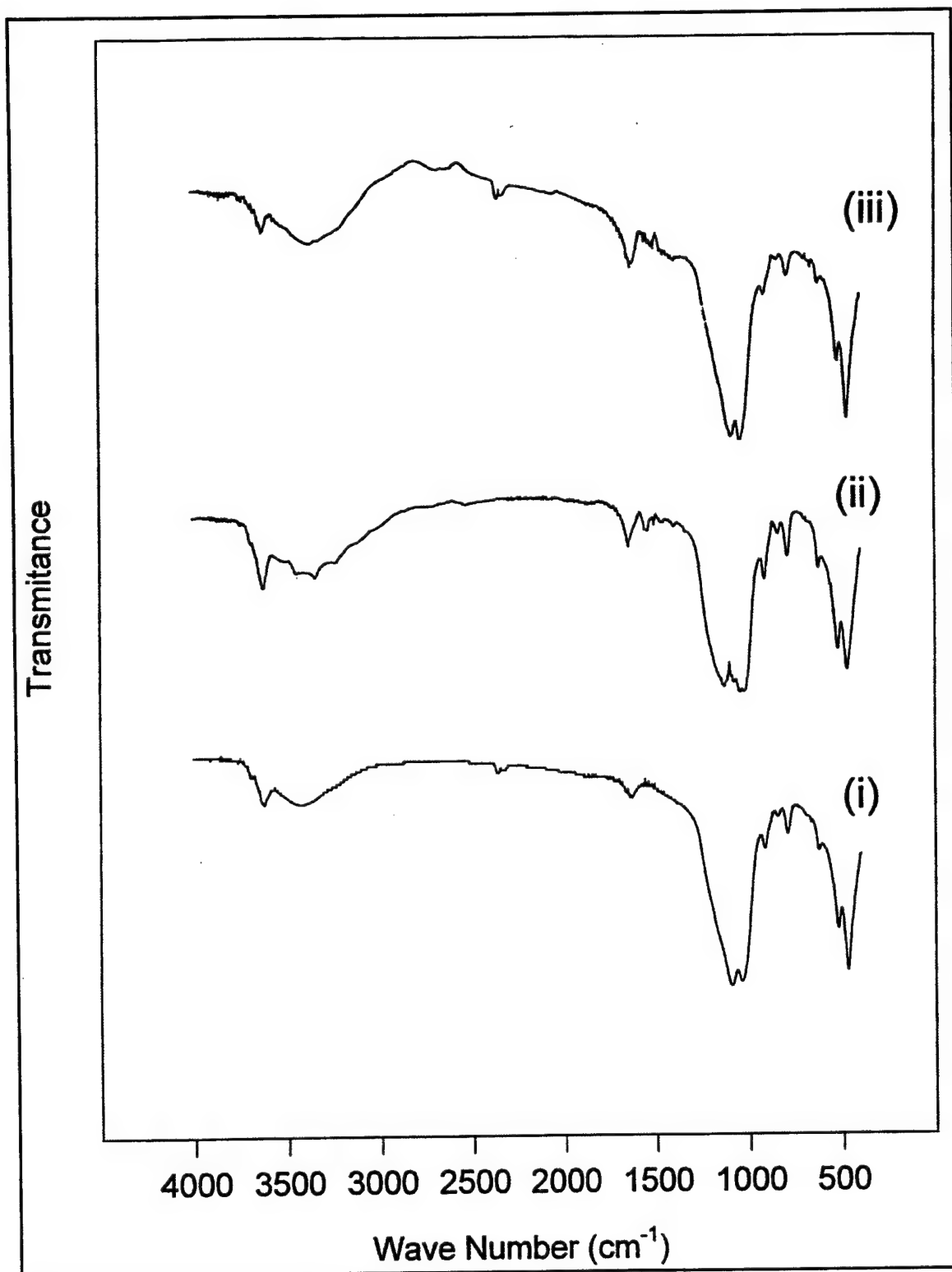STx-1 spectra, and (iii) TAT adsorbed on STx-1 minus the scaled STx-1 spectra

Figure 23. Infrared spectra: (i) STx-1, (ii) physical mixture of STx-1 and TAT minus the scaled TAT spectra, and (iii) TAT adsorbed on STx-1 minus the scaled TAT spectra

Figure 23 displays the actual IR spectrum of STx-1 (curve i) and two spectra obtained by subtracting the TAT specrum from the spectra of the two clay/TAT mixtures. The spectrum obtained by subtracting the IR spectrum of TAT-$(HCl)_3$ (Figure 22, curve i) from the IR spectrum of the TAT/STx-1 (Figure 21, curve ii) mixture is shown in Figure 23, curve ii. The spectrum obtained by subtracting the IR spectrum of TAT-$(HCl)_3$ (Figure 22, curve i) from the IR spectrum of the saturated STx-1 (Figure 22, curve iii) mixture is shown in Figure 23, curve iii. Very little difference is observed when the STx-1 spectrum (Figure 23, curve i) is compared to the dry TAT/STx-1 mixture minus the TAT-$(HCl)_3$ spectrum (Figure 23, curve ii) or the TAT-saturated STx-1 (Figure 23, curve iii). All of the spectral features are present at the same wavelengths and the intensities of the adsorptions are comparable for all three of the spectra presented in Figure 23. As noted in the discussion of the negative peak observed in Figure 22 curve iii, the peak at 3,700 in Figure 23 curve iii is small relative to the peak at the same wavelength observed in Figure 23 curves i and ii. The similarity of the IR spectrum of STx-1 and that obtained by subtracting that of the pure TAT from the TAT/STx-1 mixture and the spectrum obtained by subtracting the spectra of TAT from the TAT-saturated STx-1 suggests that no significant changes to the clay are occurring during the mixing or adsorptive processes. The reduction in adsorption of IR radiation by the hydroxide functionalities noted in Figure 23 curve iii further implicates this clay feature in the sorption of TAT and TAT transformation products.

The spectral data suggest that there is a significant difference between the physical mixture produced by grinding dry clay and TAT-$(HCl)_3$ and the compound produced when TAT in aqueous solution is loaded within the interlayer of an expandable clay. These differences can be explained by a chemical transformation of the TAT molecule within the clay, a change in the vibrational characteristics brought about by the molecule's local environment and ionic attachments, or a local environment which precludes the measurement of these frequencies. Investigations with respect to these possibilities are ongoing.

4 Summary

The role of expandable clays in the adsorption of the reductive degradation product of TNT, TAT, was investigated using purified, homoionic clays and pure TAT. It was found that this weak base produces organic cations that are capable of sorption within the interlayer of expandable clays. This adsorption resulted in an expansion of the interlayer distance between the 2:1 layers of the seven smectitic clays. XRD studies measuring the interlamellar distance of expandable clays show an expansion as contaminants are bound to the clay, indicating displacement of interlayer cations. A linear relationship was observed between the relative amount of TAT adsorbed and the interlayer spacing. A maximum expansion was achieved at between 20 and 35 weight percent TAT after which no further expansion was observed. Adsorption of TAT continued, however, with maximum adsorbances of greater than 100 mass percent observed for all seven clays. The uniformity of higher order stacking was investigated using XRD. X-ray reflections due to the higher order stacking of the clay layer increased in intensity as the amount of TAT adsorbed in the clays' interlayer increased. FTIR analysis of simple mixtures of clay and TAT and clays with intercalated TAT showed significant variations in the frequencies associated with TAT molecular motions, suggesting clay-catalyzed molecular transformation.

References

Adams, J. W., Larson, S. L., and Weiss, C. A., Jr. (1997). "Interpreting spectral effects of soil-contaminant interactions." *Selected Research in Environmental Quality FY96*. Proceedings AFOSR/ARO/WES Environmental Quality Meeting, AFOSR/NA, Bolling AFB, DC, 3-8.

Alexander, M. (1995). "How toxic are toxic chemicals in soil?," *Environ. Sci. Technol.* 29, 2713-17.

Bowman, B. T. (1973). "Effect of saturating cations on the adsorption of Dasanit®, o,o-diethyl)-[p-(methyl sulfonyl) phenyl] phosphorothioate, by montmorillinite suspensions," *J. Soil Sci. Am.* 37, 200-07.

Bowman, B. T., and Sans, W. W. (1977). "Adsorption of parathion, fenitrothion, methyl parathion, aminoparathion and paraxon by Na^+, Ca^{2+} and Fe^{3+} montmorillonite suspensions," *J. Soil Sci. Am.* 41, 514-19.

Carpenter, D. F., McCormick, N. G., Cornell, J. H., and Kaplan, A. M. (1978). "Microbial transformation of ^{14}C-labeled 2,4,6-trinitrotoluene in an activated-sludge system," *Applied Environmental Microbiology* 35(5), 949-54.

Crocker, F., Guerin, W. F., and Boyd, S. A. (1995). "Bioavailability of naphthalene sorbed to cationic surfactant-modified smectite clay," *Environ. Sci. Technol.* 29, 2953-58.

del Hoyo, C., Rives, V., and Vicente, M. A. (1996). "Adsorption of melted drugs onto smectite," *Clays and Clay Minerals* 44(3), 424-28.

Ernsten, V. (1996). "Reduction of nitrate by Fe^{2+} in clay minerals," *Clays and Clay Minerals* 44(5), 599-608.

Haderlein, S. B., and Schwarzenbach, R. P. (1993). "Adsorption of substituted nitrobenzenes and nitrophenols to mineral surfaces," *Environ. Sci. Technol.* 27, 316-26.

Haderlein, S. B., Weissmahr, K. W., and Schwarzenbach, R. P. (1996). "Specific adsorption of nitroaromatic explosives and pesticides to clay minerals," *Environ. Sci. Technol.* 30, 612-22.

Hatzinger, P. B., and Alexander, M. (1995). "Effect of aging of chemicals in soil on their biodegradability and extractability," *Environ. Sci. Technol.* 29, 537-45.

Jaynes, W. F., and Bigham, J. M. (1987). "Charge reduction, octahedral charge and lithium retention in heated, Li-saturated smectites," *Clays and Clay Minerals* 35(6), 440-48.

Jenkins, T. F. (1989). "Development of an analytical method for the determination of extractable nitroaromatics and nitroamines in soils," Ph.D. diss., University of New Hampshire, Durham, NH.

Jones, R. P. (1996). "Supercritical fluid extraction of bound explosive residues from compost," M.S. thesis, Mississippi College, Clinton, MS.

Karickhoff, S. W. (1981). "Semi-empirical estimation of sorption of hydrophobic pollutants on natural sediments and soils," *Chemosphere* 10 (8), 833-46.

Klausen, J., Tröber, S. P., Haderlein, S. B., and Schwarzenbach, R. P. (1995). "Reduction of substituted nitrobenzenes by Fe(II) in aqueous mineral suspensions," *Environ. Sci. Technol.* 29, 2396-404.

Kunyima, B., Viaene, K., Khalil, M. M. H., Schoonheydt, R. A., Crutzen, M., and De Schryver, F. C. (1990). "Study of the adsorption and polymerization of functionalized organic ammonium derivatives on a clay surface," *Langmuir* 6, 482-86.

Leggett, D. C. (1985). "Sorption of military explosive contaminants on bentonite drilling muds," CRREL Report 85-18, U.S. Army Engineer Cold Regions Research and Engineering Laboratory, Hanover, NH.

Low, P. F. (1980). "The wetting of clay: II. Montmorillonites," *Soil Sci. Soc. Amer. J.* 44, 667-76.

MacEwan, D. M. C., and Wilson, M. J. (1980). "Interlayer and intercalation complexes of clay minerals." *Crystal structures of clay minerals and their X-ray identification.* G. Brindley and G. Brown, ed., Mineralogical Society, 203.

Mercier, L., and Detellier, C. (1995). "Preparation, characterization, and applications as heavy metals sorbents of covalently grafted thiol functionalities on the interlamellar surface of montmorillonite," *Environ. Sci. Technol.* 29, 1318-23.

Moore, D., and Reynolds, R. (1989). "X-ray diffraction." *X-ray diffraction and the identification and analysis of clay minerals.* Oxford University Press, 332.

Pennington, J. (1990). "Proceedings of the sixth Corps chemists meeting, 16-17 May 1989," Miscellaneous Paper EL-90-14, U.S. Army Engineer Waterways Experiment Station, Vicksburg, MS.

Pusino, A., Gelsomino, A., and Gessa, C. (1995). "Adsorption mechanisms of imazamethabenz-methyl on homoionic montmorillonite," *Clays and Clay Minerals* 43(3), 346-52.

Pusino, A., Petretto, S., and Gessa, C. (1996). "Montmorillonite surface-catalyzed hydrolysis of fenoxaprop-ethyl," *J. Agricul. Food Chem.* 44, 1150-54.

Theng, B. K. G., Greenland, D. J., and Quirk, J. P. (1967). "Adsorption of alkylammonium cations by montmorillonite," *Clay Minerals* 7, 1-17.

Ukrainczyk, L., and Rashid, N. (1995). "Irreversible sorption of nicosulfuron on clay minerals," *J. Agricul. Food Chem.* 43(4), 855-57.

Weiss, C. A., Jr., Altaner, S. P., and Kirkpatrick, R. J. (1987). "High resolution Silicon-29 NMR spectroscopy of 2:1 layer silicates: Correlations between chemical shift, structural distortions, and chemical variations," *American Mineralogist* 72, 935-42.

Weiss, C. A., Jr., Kirkpatrick, R. J., and Altaner, S. P. (1990a). "Cesium-133 variable-temperature NMR spectroscopic study of hectorite," *Geochimica et Cosmochimica Acta* 54, 1697-1711.

_____. (1990b). "Chemical and structural variations affecting adsorbed cation sites on phyllosilicates as studied by Cesium-133 NMR," *American Mineralogist* 75, 970-82.

REPORT DOCUMENTATION PAGE

1. AGENCY USE ONLY *(Leave blank)*	2. REPORT DATE July 1998	3. REPORT TYPE AND DATES COVERED Final report	

4. TITLE AND SUBTITLE

Role of Expandable Clays in the Environmental Fate of Trinitrotoluene Contamination

5. FUNDING NUMBERS

6. AUTHOR(S)

Steven L. Larson, Charles A. Weiss, Jr., M. Rochelle Martino, Jane W. Adams

7. PERFORMING ORGANIZATION NAME(S) AND ADDRESS(ES)

U.S. Army Engineer Waterways Experiment Station
3909 Halls Ferry Road
Vicksburg, MS   39180-6199

8. PERFORMING ORGANIZATION REPORT NUMBER

Technical Report IRRP-98-6

9. SPONSORING/MONITORING AGENCY NAME(S) AND ADDRESS(ES)

U.S. Army Corps of Engineers
Washington, DC 20314-1000

10. SPONSORING/MONITORING AGENCY REPORT NUMBER

11. SUPPLEMENTARY NOTES

Available from National Technical Information Service, 5285 Port Royal Road, Springfield, VA   22161.

12a. DISTRIBUTION/AVAILABILITY STATEMENT

Approved for public release; distribution is unlimited.

12b. DISTRIBUTION CODE

13. ABSTRACT *(Maximum 200 words)*

A primary goal of the U.S. military cleanup effort is to develop technologies that can expedite the remediation of explosive contaminants in soils. Nitroaromatic explosives are known to be strongly adsorbed by soils, with as much as 20 to 50 percent of radio-labeled explosives not extractable in controlled degradation studies. This suggests that adsorption of explosives and explosives degradation products onto soil components renders them unavailable to conventional extraction methods. The mechanism of sorption to soil components has been investigated in order to properly address the ultimate fate of explosives contamination.

Trinitrotoluene undergoes reductive degradation in which nitro groups are animated to produce aminotoluene compounds. The final compound predicted by this reduction scheme is triaminotoluene. This reaction pathway results in intermediate degradation products of trinitrotoluene which act as weak bases. Protonation of these weak bases produces organic cations which are capable of sorption onto soil components. Sorption experiments were performed to determine the behavior of explosives and explosive by-products on pure clay minerals. X-ray diffraction studies measuring the interlamellar distance of expandable clays show an expansion as contaminants are bound to the clay, indicating displacement of interlayer cations. This intercalation of compounds of environmental interest within the interlamellar regions of expandable clays is an important geochemical event with implications toward a number of environmental disciplines including subsurface contaminant transport, risk assessment, contaminant bioavailability, site remediation, and natural attenuation.

14. SUBJECT TERMS

Absorption	Interlayer	Smectite
Cation exchange	Montmorillonite	Triaminotoluene
Explosives	Nontronite	
Hectorite	Saponite	

15. NUMBER OF PAGES

48

16. PRICE CODE

17. SECURITY CLASSIFICATION OF REPORT UNCLASSIFIED	18. SECURITY CLASSIFICATION OF THIS PAGE UNCLASSIFIED	19. SECURITY CLASSIFICATION OF ABSTRACT	20. LIMITATION OF ABSTRACT